

Oct 2012

# GLM-FABM

*General Lake Model (GLM) –  
Framework for Aquatic  
Biogeochemical Models (FABM)*

**Model Overview and User Documentation**  
**v0.9α**



THE UNIVERSITY OF  
WESTERN AUSTRALIA  
*Achieve International Excellence*



## Summary

This document summarises the basis and operational details for the coupled 1D lake model GLM-FABM. The General Lake Model (GLM) is a vertical stratification model able to resolve the water balance and heating and cooling of a lake system.

The Framework for Aquatic Biogeochemical Models (FABM) is a recently developed community modelling framework for simulating the biogeochemical and ecological dynamics of aquatic ecosystems. FABM supports coupling of a diverse array of water quality and ecological models to various physical 'driver' models, ranging from a 0-dimensional box model to a suite of 1, 2 or 3-dimensional hydrodynamic models. FABM has been applied to a variety of aquatic environments including oceans, estuaries and lakes.

Here we describe the conceptual basis and detailed parameterisation of the Aquatic Ecodynamics (AED) models that have developed within the FABM. The AED modules are designed as individual model 'components' that are able to be configured in a way that facilitates the user to develop custom aquatic ecosystem model configurations. Users select modules they wish to simulate and are then able to customize connections with other modules. In general, the model components consider the cycling of carbon, nitrogen, phosphorus and other relevant components such as oxygen. In addition the modules include the dynamics of organisms including different functional groups of phytoplankton and zooplankton, and their inclusion in the cycle of nutrients and organic matter.

This report summarises the models and in particular the numerical representation of the differential equations and interactions between the FABM-AED modules. A summary of typical parameter values for aquatic environments collated from a range of sources is included. The final section provides a overview of setting up and running the model. A summary of operation of the coupled GLM-FABM software is also provided.

## Authors and Contributors

### GLM

<i>Matthew R. Hipsey</i>	<i>Aquatic Ecodynamics Group, The University of Western Australia</i>
<i>Louise C. Bruce</i>	<i>Aquatic Ecodynamics Group, The University of Western Australia</i>
<i>Casper Boon</i>	<i>Aquatic Ecodynamics Group, The University of Western Australia</i>
<i>David P. Hamilton</i>	<i>The University of Waikato</i>

### FABM

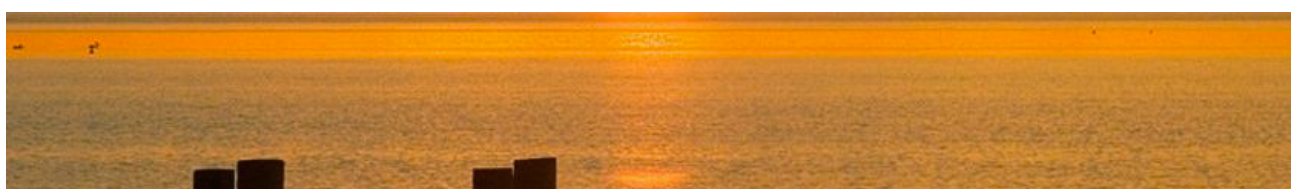
<i>Jorn Bruggeman</i>	<i>Bolding &amp; Burchard</i>
<i>Karsten Bolding</i>	<i>Bolding &amp; Burchard</i>

### AED

<i>Matthew R. Hipsey</i>	<i>Aquatic Ecodynamics Group, The University of Western Australia</i>
<i>Louise C. Bruce</i>	<i>Aquatic Ecodynamics Group, The University of Western Australia</i>
<i>Casper Boon</i>	<i>Aquatic Ecodynamics Group, The University of Western Australia</i>
<i>David P. Hamilton</i>	<i>The University of Waikato</i>

Please cite this manual as:

Hipsey, M.R., Bruce, L.C, Boon, C., Bruggeman, J., Bolding, K. & Hamilton, D.P. 2012. GLM-FABM v0.9a Model Overview and User Documentation. The University of Western Australia Technical Manual, Perth, Australia. 44pp.



# Contents

<b>SUMMARY</b>	<b>2</b>
<b>AUTHORS AND CONTRIBUTORS</b>	<b>3</b>
<b>CONTENTS</b>	<b>4</b>
<b><u>THE GENERAL LAKE MODEL (GLM)</u></b>	<b>5</b>
<b>OVERVIEW</b>	<b>5</b>
<b>MODEL DESCRIPTION</b>	<b>5</b>
Layer structure	5
Surface fluxes	5
Snow/Ice model	7
Vertical mixing	9
Inflows and outflows	10
<b>MODEL INPUT DATA REQUIREMENTS</b>	<b>10</b>
<b><u>THE FRAMEWORK FOR AQUATIC BIOGEOCHEMICAL MODELS (FABM)</u></b>	<b>12</b>
<b>OVERVIEW</b>	<b>12</b>
<b>AVAILABLE HYDRODYNAMIC DRIVER PLATFORMS</b>	<b>14</b>
<b>CANDIDATE BIOGEOCHEMICAL MODELS</b>	<b>15</b>
<b>FURTHER INFORMATION</b>	<b>15</b>
<b><u>AQUATIC ECODYNAMICS (AED) MODULE DESCRIPTIONS</u></b>	<b>16</b>
<b>OVERVIEW</b>	<b>16</b>
<b>MODULE CONCEPTUALIZATION</b>	<b>16</b>
<b>VARIABLE SUMMARY</b>	<b>20</b>
<b>MODULE DESCRIPTIONS</b>	<b>23</b>
General notation	23
Oxygen	23
Silica	24
Carbon	25
Nitrogen	26
Phosphorus	28
<b>PARAMETER SUMMARY</b>	<b>30</b>
<b><u>GLM-FABM-AED SETUP</u></b>	<b>34</b>
<b>OVERVIEW</b>	<b>34</b>
<b>INPUT FILES</b>	<b>34</b>
Physical model configuration: <code>glm.nml</code>	34
Biogeochemical model configuration: <code>fabm.nml</code>	35
Meteorology: <code>met.csv</code>	36
Inflows: <code>inflows.csv</code>	37
Outflows: <code>outflows.csv</code>	37
Biogeochemical model parameter files	38
<b>RUNNING THE MODEL</b>	<b>38</b>
<b>OUTPUTS AND POST-PROCESSING</b>	<b>38</b>
Live output plotting: <code>plots.nml</code>	39
Plotting in EXCEL	39
Plotting with PyNCview	39
Plotting with R Studio	39
Plotting in MATLAB	40
Outputting model results to <i>LakeAnalyzer</i>	40
<b><u>REFERENCES</u></b>	<b>41</b>

# The General Lake Model (GLM)

---

## Overview

The *General Lake Model* (GLM) is a one-dimensional vertical stratification hydrodynamic model driver for lakes. GLM computes vertical profiles of temperature, salinity and density by accounting for the effect of inflows/outflows, mixing and surface heating and cooling, including the effect of ice cover on heating and mixing of the lake.

Since the model is one dimensional it assumes no horizontal variability so users must ensure the lake conditions match this one-dimensional assumption. The model is ideally suited to long-term investigations ranging from seasons to decades, and for coupling with biogeochemical models to explore the role that stratification and vertical mixing play on the dynamics of lake ecosystem.

## Model Description

GLM incorporates a flexible Lagrangian layer structure similar to the approach of several 1-D lake model designs (Imberger and Patterson 1981; Hamilton and Schladow 1997; Gal et al. 2003). The Lagrangian design allows for layers to change thickness by contracting and expanding in response to inflows, outflows, mixing and surface mass fluxes. When sufficient energy becomes available to overcome density gradients, two layers will merge thus accounting for the process of mixing. Layer thicknesses are adjusted by the model in order to sufficiently resolve the vertical density gradient. Unlike the fixed grid design where mixing algorithms are typically based on vertical velocities, numerical diffusion of the thermocline is limited, making the GLM approach particularly suited to long-term investigations.

Although GLM is a new model code, many of the heating and mixing algorithms have been based on equations presented by Hamilton and Schladow (1997). GLM has been written with a modernised code structure and features a number of customisations to take advantage of recent advances in the field of numerical hydrodynamics.

### Layer structure

The model is composed of a series of layers numbered from the lake bottom to the surface. The number of layers is adjusted to maintain the assumption that each layer must have homogenous properties across the layer. Initially, the layers are assumed to be of equal thickness, and the initial number of layers,  $N_{LEV}(0)$ , depends on the user-defined minimum and maximum layer thickness limits set, and the lake depth (both defined in `glm.nml`, see model setup section). As the model progresses through time, density changes due to surface heating, vertical mixing, and inflows and outflows lead to dynamic changes in the layer structure. The number of layers will change over time, so that  $N_{LEV} = N_{LEV}(t)$ . The layer thicknesses will also change each time step as layers expand or contract, maintaining the maximum thickness required to resolve the vertical density gradient.

### Surface fluxes

The dominant drivers of stratification and mixing in most lakes are diurnal and seasonal changes in mass and energy fluxes occurring at the water-atmosphere interface. The model accounts for the surface fluxes of momentum, sensible heat and latent heat using the commonly adopted bulk aerodynamic formulae.

For momentum:

$$\tau = \rho_a C_D U_x^2$$

where  $\rho_a$  is the density of the air ( $\text{kg m}^{-3}$ ),  $C_D = 1.3 \times 10^{-3}$  and  $U_x$  is the wind velocity ( $\text{m s}^{-1}$ ) at  $x$  m above the water surface (generally assumed to be 10 m in GLM).

For sensible heat:

$$\phi_H = -\rho_a c_p C_H U_x (T_a - T_s)$$

where  $c_p$  is,  $C_H$  is the bulk aerodynamic coefficient for sensible heat transfer (=1.3e-3),  $T_a$  the air temperature ( $^{\circ}\text{C}$ ) and  $T_s$  the temperature of the surface layer ( $^{\circ}\text{C}$ ).

For latent heat:

$$\phi_E = -\rho_a C_E U_x (e_a[T_a] - e_s[T_s])$$

where  $C_E$  is the bulk aerodynamic coefficient for latent heat transfer,  $e_a$  the air vapour pressure and  $e_s$  the saturation vapour pressure at the surface layer temperature (hPa). The vapour pressure can be calculated by the following formulae:

$$e_s[T_s] = \exp \left[ 2.303 \left( 7.5 \frac{T_s}{T_s + 273.15} \right) + 0.7858 \right] \quad \text{Option 1}$$

$$e_s[T_s] = 10^{\left( 9.28603523 \frac{2322.37885 T_s}{T_s + 273.15} \right)} \quad \text{Option 2}$$

$$e_a[T_a] = \frac{RH}{100} e_s[T_a]$$

Energy fluxes to account for shortwave and longwave radiation are also included in the model. Shortwave radiation is able to penetrate according to the Beer-Lambert Law, and longwave radiation can either be specified as net flux, or incoming flux. The incoming flux may be specified directly or calculated by the model based on the cloud cover fraction and air temperature.

$$\phi_{SW}(z) = (1 - \alpha_{SW}) \hat{\phi}_{SW} \exp[-K_d z]$$

$$\alpha_{SW} = \begin{cases} 0.08 + 0.02 \sin \left[ \frac{2\pi}{365} d + \frac{\pi}{2} \right] & : \text{northern hemisphere} \\ 0.08 & : \text{equator} \\ 0.08 - 0.02 \sin \left[ \frac{2\pi}{365} d - \frac{\pi}{2} \right] & : \text{southern hemisphere} \end{cases}$$

where  $\phi_{SW}(z)$  is the short-wave radiation at depth,  $z$  (m),  $\alpha_{SW}$  is used to account for the effect of albedo on the penetration of  $\phi_{SW}$  and  $d$  is the day of the year

Long wave radiation is calculated as:

$$\phi_{LW_{in}} = \sigma [T_a + 273.15]^4 \times (1 + c_1 C) \times (1 - c_2 \exp[-c_3 T_a^2])$$

$$\phi_{LW_{out}} = \varepsilon_w \sigma [T_s + 273.15]^4$$

$$\phi_{LW_{net}} = \phi_{LW_{in}} - \phi_{LW_{out}}$$

where  $\sigma$  is the Stefan-Boltzman constant,  $C$  the cloud cover fraction (0-1),  $\varepsilon_w$  the emissivity of the water surface and constants:  $c_1 = 0.275$ ;  $c_2 = 0.261$ ;  $c_3 = 0.000777 \times 10^{-4}$ .

In addition to surface energy fluxes the model accounts for surface mass fluxes of evaporation, rainfall and snowfall ( $\text{m day}^{-1}$ ):

$$\frac{dh_s}{dt} = \lambda \phi_E + P + S$$

where  $h_s$  is the height of the surface layer (m),  $t$  time step (s),  $\lambda$  latent heat of evaporation. Note that this equation does not include changes to  $h_s$  as a result of mixing dynamics or ice formation/melt as described in the following sections.

## Snow/Ice model

The algorithms for GLM ice and snow dynamics are based on previous ice modelling studies (Patterson and Hamblin, 1988; Gu and Stefan, 1993; Rogers *et al.*, 1995; Vavrus *et al.*, 1996). To solve the heat transfer equation, the ice model uses a quasi-steady assumption that the time scale for heat conduction through the ice is short relative to the time scale of meteorological forcing (Patterson and Hamblin, 1988; Rogers *et al.*, 1995).

The steady-state conduction equations, which allocate shortwave radiation into two components, a visible ( $A_1=70\%$ ) and an infra-red ( $A_2=30\%$ ) spectral band, are used with a three-component ice model that includes blue ice, snow ice and snow (see Eq. 1 and Fig. 5 of Rogers *et al.*, 1995). Snow ice is generated in response to flooding, when the mass of snow that can be supported by the ice cover is exceeded (see Eq. 13 of Rogers *et al.*, 1995). By assigning appropriate boundary conditions to the interfaces and solving the quasi-steady state of heat transfer numerically, one can determine the upward conductive heat flux between the ice or snow cover and the atmosphere,  $\phi_0$ . The estimation of  $\phi_0$  involves the application of an empirical equation (Ashton, 1986) to estimate snow conductivity ( $K_s$ ) from its density, where the density of snow is determined as outlined in Figure 2.

At the ice (or snow) surface, a heat flux balance is employed to provide the condition for surface melting,

$$\begin{aligned}\phi_0(T_0) + \phi_{net}(T_0) &= 0 & T_0 < T_m \\ &= -\rho L \frac{dh_i}{dt} & T_0 = T_m\end{aligned}$$

where  $L$  is the latent heat of fusion (see physical constants, Table 2),  $h_i$  is the height of the upper snow or ice layer,  $t$  is time,  $\rho_i$  is the density of the snow or ice, determined from the surface medium properties,  $T_0$  is the temperature at the solid surface,  $T_m$  is the melt-water temperature ( $0^\circ\text{C}$ ) and  $\phi_{net}(T_0)$  is the net incoming heat flux, at the solid surface.

$$\phi_{net}(T_0) = \phi_{LWin} - \phi_{LWout}(T_0) + \phi_H(T_0) + \phi_E(T_0) + \phi_R(T_0)$$

where  $\phi_{LWin}$  and  $\phi_{LWout}$  are incoming and outgoing longwave radiation,  $\phi_H$  and  $\phi_E$  are sensible and evaporative heat fluxes between the solid boundary and the atmosphere, and  $\phi_R$  is the heat flux due to rainfall. These heat fluxes are calculated as above with modification for determination of vapor pressure over ice or snow (Gill, 1982) and the addition of the rainfall heat flux (Rogers *et al.*, 1995).  $T_0$  is determined using a bilinear iteration until surface heat fluxes are balanced (i.e.  $\phi_0(T_0) = -\phi_{net}(T_0)$ ) and  $T_0$  is stable ( $\pm 0.001^\circ\text{C}$ ). In the presence of ice (or snow) cover, surface temperature  $T_0 > T_m$  indicates that energy is available for melting. The amount of energy for melting is calculated by setting  $T_0 = T_m$  to determine the reduced thickness of snow or ice (as shown in Eq. 1).

Accretion or ablation of ice is determined through the heat flux at the ice-water interface,  $q_f$ . Solving for heat conduction through ice gives us:

$$q_f = q_0 - A_1 I_0 \{1 - \exp(-\lambda_{s1} h_s - \lambda_{e1} h_e - \lambda_{i1} h_i)\} - A_2 I_0 \{1 - \exp(-\lambda_{s2} h_s - \lambda_{e2} h_e - \lambda_{i2} h_i)\} - Q_{si} h_s$$

where  $I_0$  is the shortwave radiation penetrating the surface,  $\lambda$  and  $h$  are the light attenuation coefficient and thickness of the ice and snow components designated with subscripts  $s$ ,  $i$  and  $e$  for snow, blue ice and snow ice respectively, and  $Q_{si}$  is a volumetric heat flux for formation of snow ice, which is given in Eq. 14 of Rogers *et al.* (1995). In this study we fix the ice and snow light attenuation coefficients to the same values as those given by Rogers *et al.* (1995), noting the close agreement to measured values for our study lake. Reflection of shortwave radiation from the ice or snow surface is a function of surface temperature and ice and snow thickness (see Table 2, Vavrus *et al.*, 1996). Values of albedo are derived from these functions vary from 0.08 to 0.6 for ice and from 0.08 to 0.7 for snow.

The imbalance between  $q_f$  and the heat flux from the water to the ice,  $q_w$ , gives the rate of change of ice thickness at the interface with water:

$$\frac{dh_i}{dt} = \frac{q_f - q_w}{\rho_i L},$$

where  $r_i$  is the density of blue ice and  $q_w$  is given by a finite difference approximation of the conductive heat flux from water to ice:

$$q_w = -K_w \frac{\Delta T}{\Delta z},$$

where  $K_w$  is molecular conductivity and  $\Delta T$  is the temperature difference between the surface water and the bottom of the ice, which occurs across an assigned depth  $\Delta z$ . We adopt a value for  $\Delta z$  of 0.5 m, based on the reasoning given in Rogers *et al.* (1995) and the vertical resolution in our hydrodynamic model (0.125 – 1.5 m). Note that a wide variation in techniques and values is used to determine the basal heat flux immediately beneath the ice pack (e.g., Harvey, 1990).

Figure 1 shows the overall decision tree to update ice cover, snow cover and water depth. The ice cover equations are applied when water temperature first drops below 0 °C. The ice thickness is set to its minimum value of 0.05 m, which is suggested by Patterson and Hamblin (1988) and Vavrus *et al.* (1996). The need for a minimum ice thickness relates primarily to horizontal variability of ice cover during the formation and closure periods. The ice cover equations are discontinued and open water conditions are restored in the model when the thermodynamic balance first produces ice thickness < 0.05 m. The effects of snowfall, rainfall, and compaction of snow are described through appropriate choice of one of several options, depending on the air temperature and whether ice or snow is the upper boundary (Figure 1).

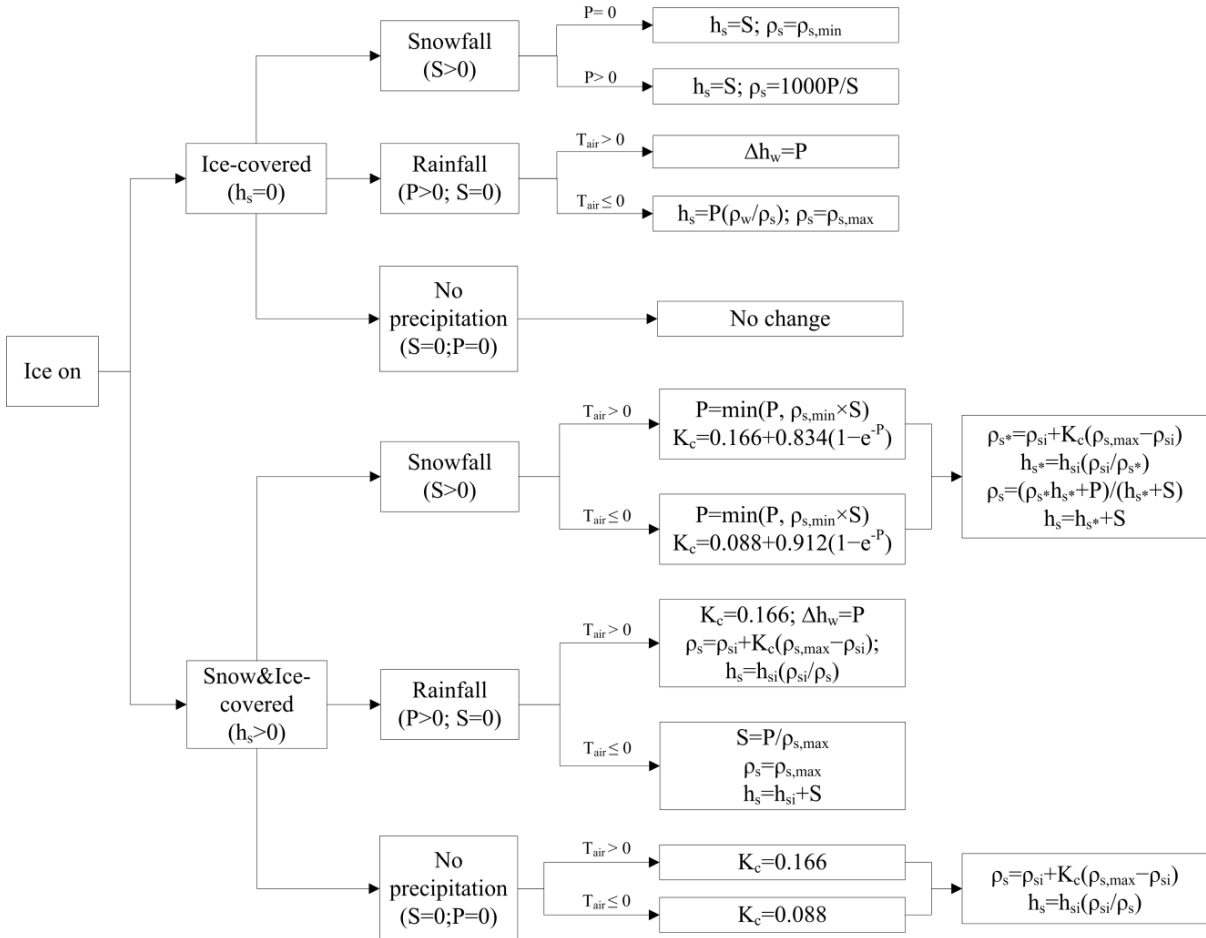


**Figure 1: Decision tree to update ice cover, snow cover and water depth according to snow compaction, rainfall ( $P$ ) and snowfall ( $S$ ) on each day, and depth of snow cover ( $h_{si}$ ) and snow density ( $\rho_{si}$ ) for the previous day. Refer to Table 1 for definitions of other variables.**

Density of fresh snowfall is determined as the ratio of measured snowfall height to water-equivalent height, with any values exceeding the assigned maximum snow density ( $r_{max} = 300 \text{ kg m}^{-3}$ ) truncated to the upper limit. The snow compaction model is based on the exponential decay formula of McKay (1968), with selection of snow compaction parameters based on air temperature (Rogers *et al.*, 1995) as well as on rainfall or snowfall. The approach of snow compaction used by Rogers *et al.* (1995) is to set the residual snow density to its maximum value when there is fresh snowfall. This method is found to produce increases in snow density that are too rapid when there is only light snowfall. As a result a gradual approach to increasing snow compaction is adopted.

### Vertical mixing

GLM works on the premise that the balance between the available energy,  $E_{TKE}$ , and the required energy to undergo mixing,  $E_{PE}$ , provides an equation for the surface mixed layer (SML) deepening rate:  $dh_{mix}/dt$ . The model calculates the available kinetic energy due to contributions from wind stirring, shear production between layers, convective overturn, and Kelvin-Helmholtz (K-H) billowing, which combined are summarised according to:

$$E_{TKE} = \underbrace{0.5C_K(w_*^2 + \psi^3 u_*^3) \Delta t}_{\substack{\text{convective overturn} \\ \text{wind stirring}}} + \underbrace{0.5 C_S \left[ u_b^2 + \frac{u_b^2 d\xi}{6 dh} + \frac{u_b \xi du_b}{3 dh} \right] h_{s-1}}_{\substack{\text{shear production} \\ \text{K-H production}}}$$

where  $u^*$  and  $w^*$  refer to the velocity scales in the horizontal and vertical respectively. The energy required to lift up water at the bottom of the mixed layer, denoted here as layer  $i-1$ , with thickness  $h_{i-1}$ , and accelerate it to the SML velocity is required for mixing to occur. This also accounts for energy consumption associated with K-H production and expressed as,  $E_{PE}$ :

$$E_{PE} = \left[ \underbrace{0.5C_T(w_*^3 + \psi^3 u_*^3)^{2/3}}_{\text{acceleration}} + \underbrace{\frac{\Delta\rho gh_{mix}}{\rho_o}}_{\text{lifting}} + \underbrace{\frac{g\xi^2}{24\rho_o} \frac{d(\Delta\rho)}{dh} + \frac{g\xi\Delta\rho}{12\rho_o} \frac{d\xi}{dh}}_{\text{K-H consumption}} \right] h_{s-1}$$

for these, the length scale of the K-H billows is summarised as:

$$\xi = \frac{\rho_o u_b^2}{g\Delta\rho}$$

and the velocity of the lower layer is approximated from:

$$u_b = \frac{u_*^2 t}{h_{mix}} + u_o$$

The model first calculates these energy arguments and then loops through layers from the top to the bottom until there is insufficient energy available to lift up the next  $i^{\text{th}}$  layer.

Mixing below the SML is modelled using a characteristic diffusivity,  $K = K_\varepsilon + K_m$ , based on

$$K_\varepsilon = \frac{\alpha_{TKE} \varepsilon_{TKE}}{N^2 + 0.6 k_{TKE}^2 u_*^2}$$

and  $K_m$  is the fixed molecular diffusivity of scalars, alpha = 0.5 and  $k$  is the wavenumber. The dissipation is calculated from

$$\varepsilon_{TKE} = \begin{cases} \epsilon & z_i < (H_t - h_{mix}) \\ \epsilon \exp \left[ -\frac{H - h_{mix} - z}{h_{sig}} \right] & z_i < (H_t - h_{mix}) \end{cases}$$

where  $h_{sig}$  is the first moment distance of the  $N^2$  distribution below  $h_{s-1}$  where  $N^2$  is the buoyancy frequency:

$$N^2 = \frac{g\Delta\rho}{(\rho)\Delta z}$$

## Inflows and outflows

Any number of inflows to the domain can be specified and these are applied at the end of the sub-daily loop, i.e. once a day. Depending on the density of the river water, the inflow will form a positive or negatively buoyant intrusion. As the inflow crosses layers it will entrain water until it reaches a level of neutral buoyancy. At its point of neutral buoyancy it is then assumed to insert as a new layer of thickness depending on the inflow volume at that time (including the effects of entrainment); it may then amalgamate with adjacent layers depending on numerical criteria within the model.

The model operates by estimating the increase in inflow thickness due to entrainment by:

$$h_i = 1.2E dx + h_{i-1}$$

where  $h_i$  is the inflow thickness,  $E$  is the entrainment rate and  $dx$  is the distance travelled by the inflowing water, calculated from the flow rate and inflow thickness. For the initial calculation:

$$h_0 = \left( 2Q_i^2 \frac{Ri}{g'} \tan^2 \beta \right)^{0.2}$$

where  $Q$  is the flow rate provided as a boundary condition,  $Ri$  is the Richardson number,  $g'$  is reduced gravity and beta is the slope of the inflow at the point where it meets the water body. The flow is estimated to increase according to:

$$Q_i = Q_{i-1} \left[ \left( \frac{h_i}{h_{i-1}} \right)^{5/3} - 1 \right]$$

and  $E$  is calculated from either:

$$E = \frac{3}{4} \left[ \frac{5 \tan \Phi}{F^2} - \frac{5C_D}{\sin \beta} \right] \frac{F^2}{(3F^2 + 2)}$$

or:

$$E = 1.6 \frac{C_D^{1.5}}{Ri}$$

where  $C_D$  is the user specified drag coefficient for the inflow and  $Ri$  of the inflow is estimated from:

$$Ri = \frac{C_D \left( 1 + 0.21C_D \sin \left[ \frac{\beta\pi}{180} \right] \right)}{\sin \left[ \frac{\beta\pi}{180} \right] \sin \left[ \frac{\Phi\pi}{180} \right] / \cos \left[ \frac{\Phi\pi}{180} \right]}$$

Outflows can be specified at any depth over the water column and they are accounted for by removing water from the layer at the depth defined at the outlet point and computation of the Grashof number:

$$Gr = \frac{N^2 A_i^2}{v^2}$$

## Model Input Data Requirements

The model requires the user to supply a hypsographic curve  $A = A(h)$  to describe the storage, elevation, area & volume relationship, meteorological time-series data for surface forcing, and daily time-series of volumetric inflow and outflow rates. Further details of the model setup and file formats are outlined in the GLM-FABM-AED Setup section. A summary of relevant parameters within the model are summarised below in Table 1.

**Table 1: GLM parameter summary.**

Symbol	Description	Units	Default value	Comment
<b>General model parameters</b>				
$h_{min}$	Minimum layer thickness	m	0.25	
$h_{max}$	Maximum layer thickness	m	0.5	
$K_w$	Extinction coefficient for shortwave radiation	$\text{m}^{-1}$	0.5	Provided by FABM if enabled
<b>Surface flux related parameters</b>				
$C_D$	Bulk aerodynamic transfer coefficient for momentum		0.0013	
$C_H$	Bulk aerodynamic coefficient for sensible heat transfer		0.0013	
$C_E$	Bulk aerodynamic coefficient for latent heat transfer		0.0013	
$\epsilon$	Emmissivity of the water surface	-	0.96	
$\sigma$	Stefan-Boltzmann constant	$\text{W m}^{-2} \text{K}^4$	5.6697e-8	
<b>Vertical mixing related parameters</b>				
$C_K$	Mixing efficiency - stirring	-	0.125	
$C_S$	Mixing efficiency – shear	-	0.2	
$C_T$	Mixing efficiency – kinetic requirement	-	0.51	
$\psi$	Relative efficiency of wind stirring vs convection	-	1.23	
$\alpha_{TKE}$	Mixing efficiency of hypolimnetic turbulence	-	0.5	Or 0.3??
<b>Inflow related parameters</b>				
$C$	Degree of inflow entrainment			
$u_{out}$	Maximum withdrawal velocity	$\text{ms}^{-1}$		
<b>Ice/Snow related parameters</b>				
$I_{e1}$	Waveband 1, snow ice light extinction	$\text{m}^{-1}$	48.0	
$I_{e2}$	Waveband 2, snow ice light extinction	$\text{m}^{-1}$	20.0	
$I_{i1}$	Waveband 1, blue ice light extinction	$\text{m}^{-1}$	1.5	
$I_{i2}$	Waveband 2, blue ice light extinction	$\text{m}^{-1}$	20.0	
$I_{s1}$	Waveband 1, snow light extinction	$\text{m}^{-1}$	6	
$I_{s2}$	Waveband 2, snow light extinction	$\text{m}^{-1}$	20	
$D_z$	Distance of heat transfer, ice water	m	0.039	
$r_e$	Density, snow ice	$\text{kg m}^{-3}$	890	
$r_i$	Density, blue ice	$\text{kg m}^{-3}$	917	
$r_s$	Density, snow	$\text{kg m}^{-3}$	Variable	
$c_{pi}$	Heat capacity, ice	$\text{kJ kg}^{-1} \text{C}^{-1}$	2.1	
$c_{pw}$	Heat capacity, ice	$\text{kJ kg}^{-1} \text{C}^{-1}$	4.2	
$K_c$	Compaction coefficient	-	Variable	
$K_e$	Thermal conductivity, snow ice	$\text{W m}^{-1} \text{C}^{-1}$	2.0	
$K_e$	Thermal conductivity, blue ice	$\text{W m}^{-1} \text{C}^{-1}$	2.3	
$K_e$	Thermal conductivity, snow	$\text{W m}^{-1} \text{C}^{-1}$	Variable	
$K_e$	Thermal conductivity, sediment	$\text{W m}^{-1} \text{C}^{-1}$	1.2	
$K_e$	Thermal conductivity, water	$\text{W m}^{-1} \text{C}^{-1}$	0.57	
$L$	Latent heat of fusion	$\text{kJ kg}^{-1}$	0334	

# The Framework for Aquatic Biogeochemical Models (FABM)

---

## Overview

The *Framework for Aquatic Biogeochemical Models* (FABM) is a relatively new state-of-the-art code-base for the simulation of aquatic biogeochemical and ecological dynamics. It has been developed in response to deficiencies in existing rigid water quality modelling approaches as much present-day software does not address the challenges faced in model coupling (for example see discussion in Arhonditsis et al. 2006, and Mooij et al. 2010) as well as a recognized need to develop improved standards and flexibility in model integration in concert with an active development community (Trolle et al., 2012). The basic framework has been developed by Dr. Jorn Bruggeman and colleagues under the EU7 project “Marine Ecosystem Evolution in a Changing Environment” (MEECE), and readers are referred to Bruggeman (2011) for further background.

FABM itself is not a water quality model, but rather it is a sophisticated code framework that supports a common library of biogeochemical and ecological models and model ‘components’. It has been designed to facilitate integration of different biogeochemical/ecological model approaches (both process-based and empirical), model currencies and to enable coupling with a diverse array of physical (hydrodynamic) driver models. Therefore, its intention is not to be a sophisticated “model of everything” and users can configure it to be as simple or as complicated as desired.

The underlying framework allows a flexible coupling interface to hydrodynamic models, and at its core it consists of a thin layer of code designed to manage communication and data exchange, via programming interfaces through which a physical host (hydrodynamic model) and any number biogeochemical models pass information. It has since been adopted across the science community having been applied to numerous types of aquatic systems ranging from the global ocean (coupled to MOM4 and GOTM), to estuaries and rivers (coupled to GETM), and to lakes (coupled to GLM, a 1D lake model). It is currently being coupled with both TUFLOW Classic and TUFLOW-FV as part of a collaborative project between BMT-WBM and UWA to provide a comprehensive river-floodplain-estuary modelling platform. The model adopts a standard interface so that the code itself can be coupled with other forms of hydrodynamic models, or it can be run in isolation (0D) for hypothesis testing and ecological model prototyping. The advantage of the FABM approach over other platforms is its flexibility for coupling a diverse array of model approaches and its support for rigorous numerical solution schemes (eg. Burchard et al. 2005; Broekhuizen et al. 2008) that are known to be important in achieving accurate solutions of complex biogeochemical model equation sets. Its code structure is also designed to improve speedup? when used with parallel processors.

FABM itself supports custom model configurations and currently includes common biogeochemical configurations such as the ‘Fasham’ model template (currently the most highly cited aquatic biogeochemical model approach; Arhonditsis et al. 2006), as well as simple ‘NPZD’ model templates (eg. Burchard et al. 2006). However, it is easily customisable to simulate biogeochemical and ecological conditions as required, and in particular it is possible to develop configurations specific to any systems where standard eutrophication model templates may not be ideal. To this end, the “*Aquatic Ecodynamics*” (AED) library of model components has been developed and implemented within the FABM framework (Figure 1), and is the main subject of this summary. For more information on the code structure and approach of FABM the reader is referred to Bruggeman et al (2011), and to Trolle et al. (2012) for discussion around the philosophy underlying the development of the framework approach.

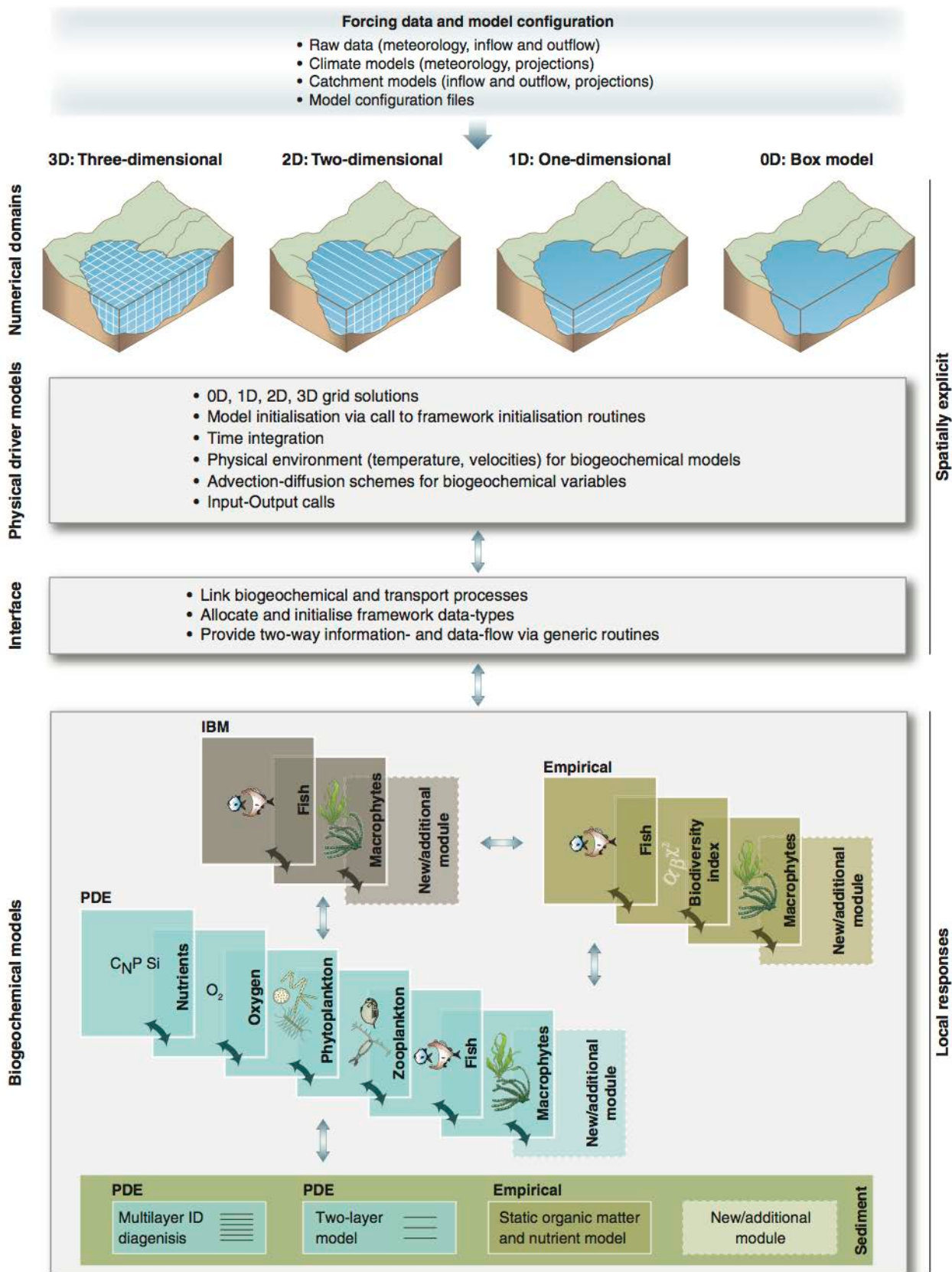


**Figure 2: Schematic representation of coupling and biogeochemical modelling approach, taken from Trolle et al. (2012).**

## Available hydrodynamic driver platforms

**Table 2: Current driver models linked to FABM.**

Model	Dimensionality & grid structure	Stratification & Vertical Mixing	Comments
0D Driver	0D	-	Simple 'box' model for testing biogeochemical model operation
General Ocean Turbulence Model ( <b>GOTM</b> )	1D	Library of range of simple and complex mixing approaches	<a href="http://www.gotm.net">http://www.gotm.net</a>
General Estuarine Transport Model ( <b>GETM</b> )	3D structured grid, with curvilinear option	Uses GOTM turbulence library	<a href="http://www.getm.eu">http://www.getm.eu</a>
Modular Ocean Model version 4 ( <b>MOM4</b> )	3D		<a href="http://www.gfdl.noaa.gov/fms">http://www.gfdl.noaa.gov/fms</a>
General Lake Model ( <b>GLM</b> )	1D (vertical) – Lagrangian layered grid	Custom vertical mixing algorithms	Includes Ice cover  Daily and sub-daily time-step supported;  Simple to use  Reimplementation of Hamilton and Schladow, 1997)
TUFLOW-FV	2D/3D- Flexible mesh in horizontal, and sigma or z-coordinate in vertical	Uses external turbulence libraries for vertical mixing	<a href="http://www.tuflow.com">www.tuflow.com</a>  Available 2012/2013

## Candidate biogeochemical models

There are currently a range of ecosystem models that are implemented within the FABM framework, that vary in complexity and can be applied to model a range of different ecosystem contexts. These are summarised briefly in Table 3, and since the focus of this document is the AED models, readers are referred to the references for details of the other models. Note this list is constantly expanding and other models are frequently added to the FABM code-base.

**Table 3: Current coupled aquatic biogeochemical models included within the FABM framework.**

Name	Description
<i>pml/ carbonate</i>	Carbonate chemistry
<i>pml/ ersem</i>	European Regional Seas Ecosystem Model
<i>metu/ mnemiopsis</i>	population model for Mnemiopsis
<i>gotm/ npzd</i>	Simple NPZD model (Burchard et al., 2005), ported from GOTM
<i>gotm/ fasham</i>	Fasham et al. (1990) model with modifications by, ported from GOTM
<i>iow/ ergom</i>	Baltic Sea Research Institute ecosystem model
<i>aed/ ...</i>	<i>Aquatic Ecodynamics Library</i> (focus of this report, described in the next section)
<i>examples/ benthic</i>	Example of a benthic predator

## Further information

FABM documentation, code and test cases are currently available from a Git repository at SourceForge:  
<http://fabm.sourceforge.net>.

The contents of this repository can be obtained on UNIX/Linux/Mac OS X systems by executing:

```
git clone git://fabm.git.sourceforge.net/gitroot/fabm/fabm
```

and users on windows can use one of several available GIT clients.

# Aquatic Ecodynamics (AED)

## Module Descriptions

---

### Overview

The philosophy of the AED modules within FABM is that individual model ‘components’ can be configured in a way that facilitates custom aquatic ecosystem configurations. Users select modules they wish to simulate and then are able to customize connections with other modules. The modules exist within a hierarchy of dependencies, and connections must be set in the right order. In general, model components consider the cycling of carbon, nitrogen and phosphorus, and other relevant components such as oxygen, and are able to simulate organisms including different functional groups of phytoplankton and zooplankton, and also organic matter.

Much of the science basis and mathematical approach implemented in the AED modules is similar to aquatic ecological models that have been used over the past two decades, including lake analysis by Hamilton and Schladow (1997), and analysis using CAEDYM (Bruce et al. 2006; Gal et al., 2009; Spillman et al., 2007, 2008). The AED modules, however, are implemented within the FABM numerical framework and include numerous different process representations beyond these earlier studies, as reported in detail below.

### Module conceptualization

Whilst the AED modules are highly flexible and can be customised for user-defined biogeochemical and ecological configurations, they have generally been designed to simulate the interactions between nutrients, organic matter, phytoplankton and zooplankton. When coupled with the hydrodynamic driver, the modules allow for a comprehensive simulation of processes that govern the transport and fate of water quality attributes included suspended sediment, dissolved inorganic nutrients, organic matter (dissolved and particulate), phytoplankton and zooplankton, and relevant fluxes at the air-water and sediment-water interface. Given the flexible nature of FABM model integration, multiple identical modules can be simulated allowing the user to further partition ecological components. For example, two alternative organic matter modules can be simulated, each with unique parameters that reflect labile versus refractory material. Similarly, multiple phytoplankton sub-modules can be configured to allow for either groups of functional types or groups of similar species to be simulated.

The modules together simulate the C, N, P, DO, and Si cycles including inorganic nutrient, organic matter, phytoplankton, and zooplankton. In a typical application around three phytoplankton groups (bacillariophytes or diatoms, D; chlorophytes or green algae, G; cyanobacteria or blue-green algae, B) would be simulated with or without zooplankton. For this configuration, nine state variables are required to model the algal biomass ( $A_D$ ,  $A_G$ ,  $A_B$ ) if the dynamically calculated internal nutrient stores of N ( $PHY\_N_D$ ,  $PHY\_N_G$ ,  $PHY\_N_B$ ) and P ( $PHY\_P_D$ ,  $PHY\_P_G$ ,  $PHY\_P_B$ ), and five dissolved inorganic nutrients (FRP, NO<sub>3</sub>, NH<sub>4</sub>, PIP, RSi), three dissolved (DOC, DON, DOP) and three particulate (POC, PON, POP) detrital organic matter groups, and dissolved oxygen (DO). In the absence of zooplankton this constitutes around 22 state variables, all of which are mixed, transported and subject to boundary forcing by the hydrodynamic driver (Table 1). Although the model allows simulation of multiple organic matter variables to resolve labile and refractory components, only one set of organic matter state variables are described here as often monitoring data is insufficient to justify resolving organic pools into their components.

A general summary of the key modules is included below and detailed equations, parameter descriptions and typical values used are presented in the following section.

**Light** - The hydrodynamic driver supplies incident shortwave radiation, (used in surface thermodynamics calculations), to FABM. For primary production, the shortwave (280-2800 nm) intensity at the surface is converted to the photosynthetically active component (PAR) based on the assumption that 45% of the incident spectrum lies between 400-700 nm (eg. Jellison and Melack, 1993). PAR penetrates into the water column according to the Beer-Lambert Law with the light extinction coefficient dynamically adjusted to account for variability in the concentrations of algal,

inorganic and detrital particulates, and dissolved organic carbon based on user defined specific attenuation coefficients.

**Dissolved Oxygen** - DO dynamics account for atmospheric exchange, sediment oxygen demand, microbial use during organic matter mineralisation and nitrification, photosynthetic oxygen production and respiratory oxygen consumption, and respiration by other optional biotic components. Atmospheric exchange is based on the model of Wanninkhof (1992) and the flux equation of Riley and Skirrow (1974). A simple sediment oxygen demand flux is currently implemented that varies as a function of the overlying water temperature and dissolved oxygen levels. Microbial activity facilitates the breakdown of organic carbon (in particular, DOC) to CO<sub>2</sub>, and a stoichiometrically equivalent amount of oxygen is removed. The process of nitrification also requires oxygen and is dependent on the half-saturation constant for the effect of oxygen limitation calculated using the stoichiometric factor for the ratio of oxygen to nitrogen. Photosynthetic oxygen production and respiratory oxygen consumption is simulated for each of the simulated phytoplankton groups.

**Carbon, Nitrogen, Phosphorus and Silica** - Both the inorganic and organic, and dissolved and particulate forms of C, N and P are modelled explicitly along the degradation pathway of POM to DOM to dissolved inorganic matter (DIM). The decomposition and mineralisation process varies in response to temperature, and can be configured to slow down as oxygen becomes limiting. The nitrogen cycle includes additional processes of denitrification, nitrification and N<sub>2</sub> fixation. N<sub>2</sub> levels however are not tracked as a specific state variable. The phosphorus cycle also accounts for adsorption/desorption of PO<sub>4</sub> onto suspended solids (SS), and adopts the Langmuir isotherm model as implemented by Chao et al (2010).

The silica cycle is simpler and includes the processes of biological uptake of dissolved Si (RSi) by diatoms into the internal Si (ISi) pool, dissolved sediment fluxes of RSi, diatom mortality directly into the RSi sediment pool, settling of ISI. This relatively simple representation assumes that diatom frustules rapidly mineralise.

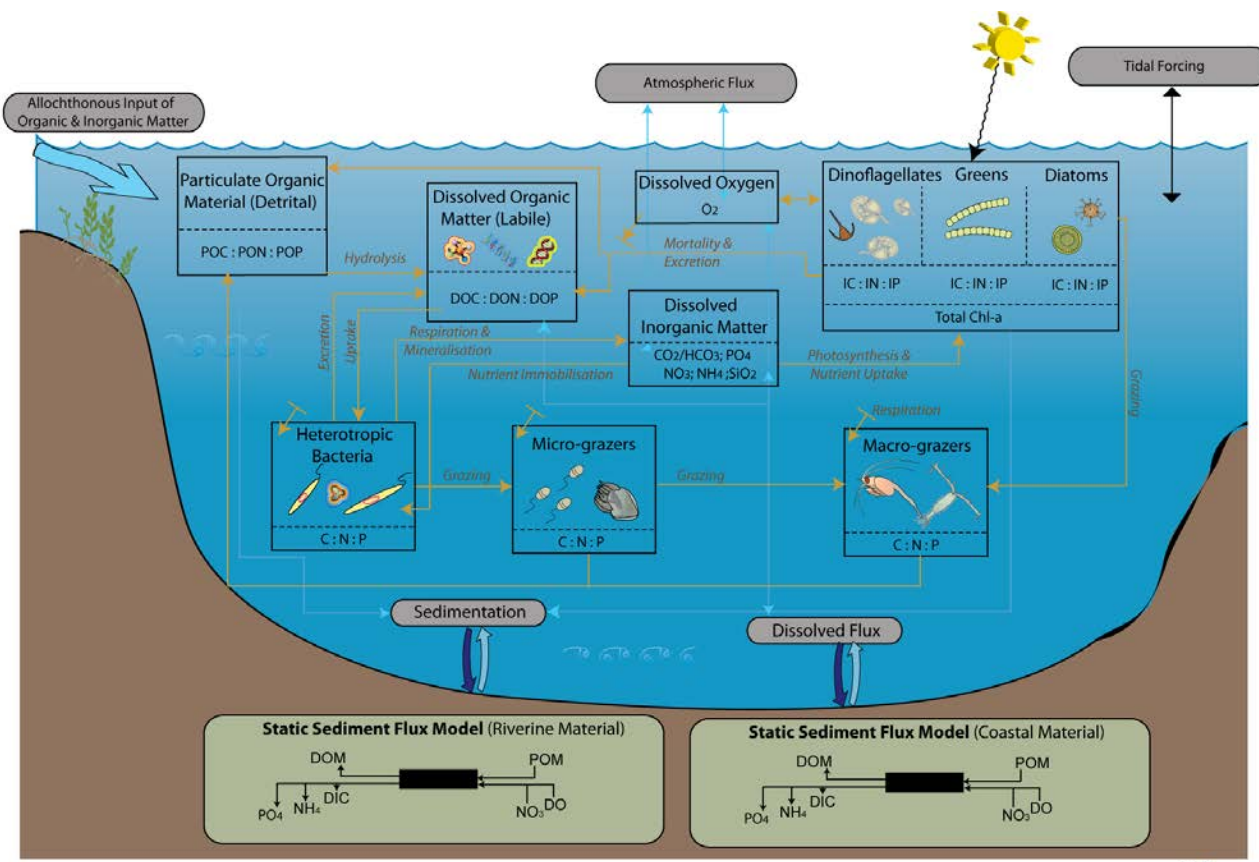


Figure 3: AED module conceptual model of carbon and nutrient flux pathways and planktonic groups.

**Phytoplankton Dynamics** - phytoplankton groups are configurable within FABM that are generic, with any configurable to include internal silica stores if desired (eg., for simulating diatoms). The algal biomass of group  $a$ ,  $PHY\_C_a$ , is simulated in units of carbon ( $\text{mmol C m}^{-3}$ ), and the group can be configured to have a constant C:N:P ratio, or have dynamic uptake of C:N:P in response to changing water column and intra-cellular processes. For each phytoplankton group, the maximum potential growth rate at  $20^\circ\text{C}$  is multiplied by the minimum value of expressions for limitation by light, phosphorus, nitrogen and silica when diatoms are considered. While there may be some interaction between limiting factors, a minimum expression is likely to provide a realistic representation of growth limitation (Rhee and Gotham, 1981).

The level of light limitation on phytoplankton growth can be configured to be subject to photoinhibition or to be non-photoinhibited. In the absence of significant photoinhibition, the model of Webb et al. (1974) is used to quantify the fractional limitation of the maximum potential rate of carbon fixation if light saturation behavior was absent (Talling, 1957), and the equations are analytically integrated with respect to depth. For the case of photoinhibition, the light saturation value of maximum production ( $I_S$ ) is used and the net level effect is averaged over the cell by integrating over depth.

To allow for reduced growth at non-optimal temperatures, a temperature function is used where the maximum productivity occurs at a temperature  $T_{OPT}$ ; above this productivity decreases to zero at the maximum allowable temperature,  $T_{MAX}$ . Below the standard temperature,  $T_{STD}$  the productivity follows a simple Arrhenius scaling formulation. In order to fit a function with these restrictions the following conditions are assumed: at  $T = T_{STD}$ ,  $\Phi_{tem}(T)=1$  and at  $T = T_{OPT}$ ,  $\frac{d\Phi_{tem}(T)}{dT} = 0$ , and at  $T = T_{MAX}$ ,  $\Phi_{tem}(T) = 0$ . This can be numerically solved using Newton's iterative method and can be specific for each phytoplankton group.

Metabolic loss of nutrients from mortality and excretion is proportional to the constant internal nitrogen to chla ratio multiplied by the loss rate and the fraction of excretion and mortality that returns to the detrital pool. Loss terms for respiration, natural mortality and excretion are modelled with a single 'respiration' rate coefficient. This loss rate is then divided into the pure respiratory fraction and losses due to mortality and excretion. The constant  $f_{DOM}$  is the fraction of mortality and excretion to the dissolved organic pool with the remainder into the particulate organic pool.

There are two options to model the P, N and C dynamics within the algal groups: a constant nutrient to carbon ratio, or dynamic intracellular stores. For the first model a simple Michaelis-Menten equation is used to model nutrient limitation with a half-saturation constant for the effect of external nutrient concentrations on the growth rate as for RSi in this application.

The internal phosphorus and nitrogen dynamics within the phytoplankton groups can be modelled using dynamic intracellular stores that are able to regulate growth based on the model of Droop (1974). This model allows for the phytoplankton to have dynamic nutrient uptake rates with variable internal nutrient concentrations bounded by user-defined minimum and maximum values. Nutrient losses through mortality and excretion for the internal nutrient model are similar to the simple model described above, except that the dynamically calculated internal nutrient concentrations are used.

For diatom groups modelled, silica processes that are modeled include uptake of dissolved silica, an internal store of silica, and loss through mortality and excretion. The silica limitation function for diatoms is similar to the constant cases for nitrogen and phosphorus.

**Zooplankton Dynamics** - Net zooplankton growth is calculated as a balance between food assimilation and losses from respiration, excretion, egestion, predation and mortality. Net grazing is calculated as the product of the maximum potential rate of grazing, assimilation efficiency and temperature and food limitation functions. Loss terms are added to each of the selected prey state variables in proportional to user defined preference factors and food availability. These loss terms include particulate nitrogen and phosphorus when particulate carbon is included in the prey list. Similarly for internal phytoplankton nutrients when dynamic internal nutrients are simulated.

Positive flux to the particulate C:N:P pools includes the sum of assimilation factor (to account for messy feeding) and a user defined fraction of total loss to account for the production of fecal pellets. A constant internal nutrient ratio is

assumed for simplicity, and since the various input and output fluxes have variable C:N:P ratios, the excretion of dissolved organic C:N:P is dynamically adjusted each time-step to maintain this ratio.

**Water Column Geochemistry** - The module allows the user to input any inorganic components of interest (e.g. ions, metals) and account for any pure phases (i.e. minerals, gases) and the aed\_geochemistry module will solve speciation of the complete system based on a thermodynamic equilibrium. Optional kinetic processes may also be configured through dedicated modules, such as microbially mediated redox transformations in aed\_carbon, aed\_iron and aed\_sulfur. Like all variables the geochemical components are subject to transport and mixing and are influenced by biological processes, such as photosynthesis, nutrient uptake and organic matter mineralisation. These will dynamically effect the aqueous speciation and pH. Atmospheric and sediment transfers of relevant geochemical components are also configurable. The geochemical model is similar to that used for mine lakes impacted by acid mine drainage (Oldham *et al.*, 2009) and other fresh and saline pH neutral waters (eg. Hipsey and Busch, 2012).

**Sediments and Resuspension** – Static and dynamic sediment diagenesis models have been included within the AED FABM modules, which allow for prediction of oxygen, nutrient and metals fluxes at the sediment water-interface. These may be spatially variable and can be managed through the aed\_sedflux interface module.

In summary, currently the modules support the following, and they are presented here in order of hierarchical dependence, which is important in setting the order of module configuration in the fabm.nml control file:

**aed\_tracer:**

- Passive tracer, with optional decay rate
- Sedimentation, and benthic flux

**aed\_turbidity:**

- Simple particle model with discrete size classes
- Sedimentation included and light attenuation affect

**aed\_iron:**

- Particulate and dissolved components
- Benthic flux
- Oxidation and photo-reduction

**aed\_silica**

- benthic flux
- phytoplankton uptake

**aed\_oxygen:**

- Surface/bottom exchange
- Photosynthesis / respiration
- OM mineralization consumption (BOD)

**aed\_carbon:**

- Surface/bottom exchange of DIC and CH<sub>4</sub>
- Photosynthesis / respiration contribution
- OM mineralization production of DIC

**aed\_phosphorus**

- benthic flux of PO<sub>4</sub>
- phytoplankton uptake
- organic matter mineralisation
- adsorption to particles

**aed\_nitrogen**

- benthic flux of NO<sub>3</sub> and NH<sub>4</sub>
- phytoplankton uptake
- denitrification/nitrification
- organic matter mineralisation

**aed\_organicmatter**

- POM and DOM for C, N, and P
- Decomposition and hydrolysis of detrital material, and mineralisation
- Benthic flux of dissolved organic material
- phytoplankton production through excretion, exudation and mortality
- Multiple “pools” can be configured (eg. labile/refractory)

**aed\_chla:**

- generic bulk phytoplankton module for simulating growth of chl-a

**aed\_phytoplankton:**

- Multiple groups, support flexible setting of interactions and configuration (eg. N uptake of NH<sub>4</sub>, NO<sub>3</sub>, DON, N<sub>2</sub> possible)
- Inclusion of `aed_phyto_pars.nml` which stores many pre-configured parameter sets that users can choose from
- general library of temp, light, nutrient environmental dependencies
- Variable IN:IP (droop) or fixed N:P (static) allowed

**aed\_zooplankton:**

- Multiple groups can be configured to represent species/functional groups or size classes within species/functional groups.
- Physiological parameters set by user in name list `aed_zoop_params.nml`.
- Choice of food and preference factors set in name list from phytoplankton, zooplankton, bacteria and particulate organic matter

**aed\_totals:**

- Module to allow derived parameters for TN, TP and TSS

**aed\_geochemistry:**

- Aqueous speciation and calculation of pH and ionic strength
- Precipitation / dissolution of mineral phases
- Can link and include state variables from all other modules (eg. Fe, DIC etc)
- Suitable for non-neutral conditions

**aed\_sedflux:**

- Generic benthic exchange module for interfacing between the sediment and water column

**aed\_seddiagenesis:**

- Depth resolved sediment advection-diffusion-reaction model

## Variable summary

All the possible state variables that can be simulated the AED modules are listed in Table X. Although there are numerous state variables in total, many are not compulsory and depend on the modules selected and how the interactions between modules are configured. For a simple water quality simulation the variables there is a minimum configuration of DO, DOM, POM, PO<sub>4</sub>, NH<sub>4</sub> and NO<sub>3</sub>, and phytoplankton/chlorophyll-a are available. However, these are not compulsory if the user simply wishes to model pathogens or suspended sediment for example. They are configured via options outlined in the `fabm.nml` file.

Each of the variables listed below can also be specified as an output via the NetCDF output. They are generally available as a suffix to the module name, `aed_module_varname`, for example, to view oxygen search for the `aed_oxygen_oxy`. The keywords for most of the simulated variables are also used to specify the inflow boundary conditions in relevant inflow files (depending on the hydrodynamic driver).

**Table 4: Current coupled aquatic biogeochemical models included within the FABM framework.**

Symbol	Name	Units	AED module
<b>General</b>			
$t$	= time	days	
$dz$	= layer height	m	
$A$	= layer/cell area	$\text{m}^2$	
<b>Environmental dependencies</b>			
$T$	Temperature	$^\circ\text{C}$	
$S$	Salinity	ppt	
$I_{PAR}$	Photosynthetically active radiation (PAR: 400-700nm)	$\text{W}/\text{m}^2$	
<b>Oxygen</b>			
$O_2$	= concentration of dissolved oxygen	$\text{mmol O}/\text{m}^3$	aed_oxygen
<b>Silica</b>			
$RSi$	= reactive silica ( $\text{SiO}_2$ ) concentration	$\text{mmol Si}/\text{m}^3$	aed_silica
<b>Carbon</b>			
$DIC$	= concentration of inorganic carbon	$\text{mmol C}/\text{m}^3$	aed_carbon
$pH$	= pH	$\text{mmol C}/\text{m}^3$	aed_carbon
$CH4$	= concentration of methane	$\text{mmol C}/\text{m}^3$	aed_carbon
<b>Nitrogen</b>			
$NH_4$	= concentration of ammonium	$\text{mmol N}/\text{m}^3$	aed_nitrogen
$NO_3$	= concentration of nitrate	$\text{mmol N}/\text{m}^3$	aed_nitrogen
$TN$	= concentration of total nitrogen	$\text{mmol N}/\text{m}^3$	aed_totals
<b>Phosphorus</b>			
$PO_4$	= concentration of filterable reactive phosphorus ( $\text{PO}_4$ )	$\text{mmol P}/\text{m}^3$	aed_phosphorus
$PO_4^{ads}$	= concentration of adsorbed phosphate	$\text{mmol P}/\text{m}^3$	aed_phosphorus
$TP$	= concentration of total phosphorus	$\text{mmol P}/\text{m}^3$	aed_totals
<b>Organic Matter (DOM &amp; POM)</b>			
$POC$	= concentration of particulate organic carbon	$\text{mmol C}/\text{m}^3$	aed_organic_matter
$DOC$	= concentration of dissolved organic carbon	$\text{mmol C}/\text{m}^3$	aed_organic_matter
$PON$	= concentration of particulate organic nitrogen	$\text{mmol N}/\text{m}^3$	aed_organic_matter
$DON$	= concentration of dissolved organic nitrogen	$\text{mmol N}/\text{m}^3$	aed_organic_matter
$POP$	= concentration of particulate organic phosphorus	$\text{mmol P}/\text{m}^3$	aed_organic_matter
$DOP$	= concentration of dissolved organic phosphorus	$\text{mmol P}/\text{m}^3$	aed_organic_matter
<b>Phytoplankton</b>			
$N_{PHY}$	= number of simulated phytoplankton groups		aed_phytoplankton
$PHY\_C$	= concentration of phytoplankton carbon	$\text{mmol C}/\text{m}^3$	aed_phytoplankton
$PHY\_N$	= concentration of phytoplankton nitrogen	$\text{mmol N}/\text{m}^3$	aed_phytoplankton
$PHY\_P$	= concentration of phytoplankton phosphorus	$\text{mmol P}/\text{m}^3$	aed_phytoplankton
$PHY\_Si$	= concentration of phytoplankton silica	$\text{mmol Si}/\text{m}^3$	aed_phytoplankton
<b>Zooplankton</b>			
$N_{zoo}$	= number of simulated zooplankton groups		aed_zooplankton
$ZOO$	= concentration of zooplankton carbon	$\text{mmol C}/\text{m}^3$	aed_zooplankton
<b>Geochemistry</b>			
$pH$	= pH	-	aed_carbon or aed_geochemistry

<i>ubalchg</i>	= unbalanced charge concentration	meq	aed_geochemistry
<i>DIC</i>	= concentration of dissolved inorganic carbon	mmol C/m <sup>3</sup>	aed_carbon or aed_geochemistry
<i>CH4</i>	= concentration of methane	mmol C/m <sup>3</sup>	aed_carbon or aed_geochemistry
<i>Ca</i>	= concentration of calcium	mmol Ca/m <sup>3</sup>	aed_geochemistry
<i>Na</i>	= concentration of sodium	mmol Na/m <sup>3</sup>	aed_geochemistry
<i>Mg</i>	= concentration of magnesium	mmol Mg/m <sup>3</sup>	aed_geochemistry
<i>Cl</i>	= concentration of chloride	mmol Cl/m <sup>3</sup>	aed_geochemistry
<i>SO4</i>	= concentration of sulfate	mmol SO <sub>4</sub> /m <sup>3</sup>	aed_sulfur or aed_geochemistry
<i>FeII</i>	= concentration of dissolved ferrous iron	mmol FeII/m <sup>3</sup>	aed_iron or aed_geochemistry
<i>FeIII</i>	= concentration of dissolved ferric iron	mmol FeIII/m <sup>3</sup>	aed_iron or aed_geochemistry
<i>Al</i>	= concentration of dissolved aluminum	mmol Al/m <sup>3</sup>	aed_geochemistry
<i>CaCO<sub>3(s)</sub></i>	= concentration of calcite	mmol /m <sup>3</sup>	aed_geochemistry
<i>FeOH3(s)</i>	= concentration of iron hydroxide	mmol /m <sup>3</sup>	aed_iron or aed_geochemistry
<i>Al(OH)3(s)</i>	= concentration of gibbsite	mmol /m <sup>3</sup>	aed_geochemistry
...others as configured			
<b>Sediment</b>			
<i>F<sub>sedO<sub>2</sub></sub></i>	= Spatially variable sediment flux of oxygen	mmol O <sub>2</sub> /m <sup>2</sup> /day	aed_sedflux
<i>F<sub>sedPO<sub>4</sub></sub></i>	= Spatially variable sediment flux of phosphate	mmol P /m <sup>2</sup> /day	aed_sedflux
<... TBC>	= sediment O <sub>2</sub> concentration	mmol O <sub>2</sub> /m <sup>3</sup>	aed_seddiagenesis
	= sediment PO <sub>4</sub> concentration	mmol P/m <sup>3</sup>	aed_seddiagenesis
	....40 more...		
<b>Turbidity</b>			
<i>N<sub>SS</sub></i>	= number of simulated solids groups		aed_turbidity
<i>C<sub>SS</sub></i>	= suspended solids group concentration	g /m <sup>3</sup>	aed_turbidity
<i>TSS</i>	= total suspended solids concentration	g/m <sup>3</sup>	aed_totals
<b>Pathogens</b>			
<i>N<sub>PATH</sub></i>	= number of simulated pathogen groups		aed_pathogens
<i>C<sub>PATH</sub></i>	= pathogen group concentration	orgs /m <sup>3</sup>	aed_pathogens

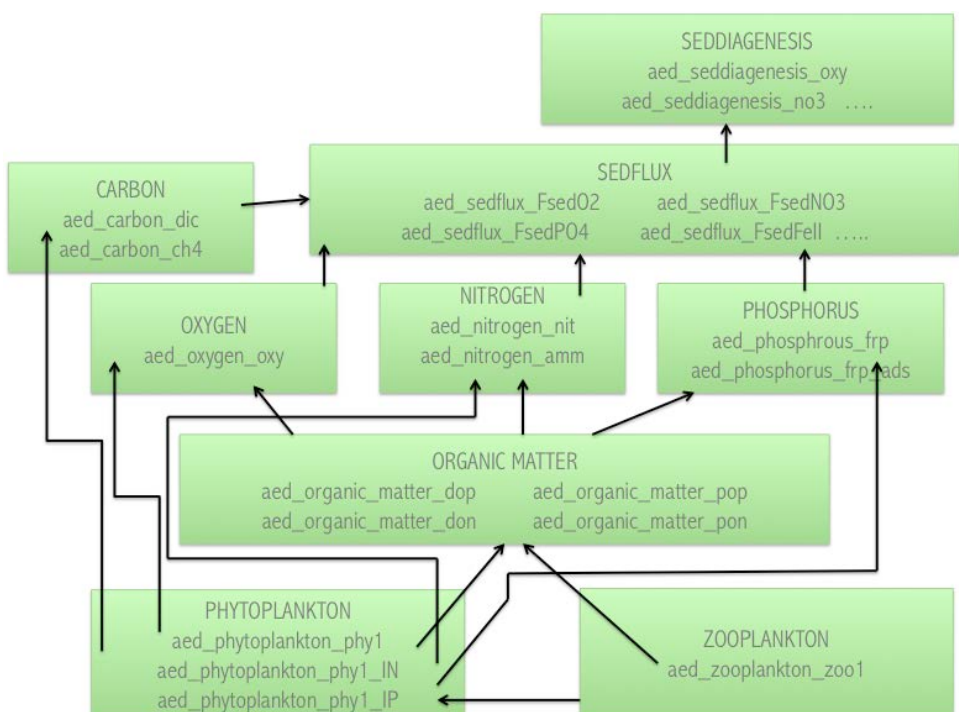


**Figure 4: Example of connections between AED modules and module variables.**

## Module descriptions

In this section the detailed model mass balance and biogeochemical algorithms are described. These are not organized by AED modules, but rather based on the element or ecosystem component in line with the conceptual model.

Note that all balance equations in effect also have terms for advection, dispersion, turbulent mixing, and inflows and outflow boundary conditions, however these are highly specific to the particular to the hydrodynamic driver being used to run the FABM-AED model. Due to potential differences between them, they are not included in the below expressions and the equations presented here solely focus on biogeochemical and ecological interactions.

### General Notation

$N$	= number of groups [integer]
$a, om, z$	= indices of various sub-groups of algae/phytoplankton, organic matter and zooplankton [integer]
$\chi_{C:Y}^{group}$	= the stoichiometric ratio of “group” between C and element “Y” [mmol C/mmol Y]
$f_{process}^{var}$	= function that returns the mass flux of “process” on “var” [mmol var/time]
$R_{process}^{var}$	= the rate of “process” influencing the variable “var” [/time]
$F_{max}^{var}$	= the maximum benthic areal flux of variable “var” [mmol var/area/time]
$p_{source}^{group}$	= the preference of “group” for “source” [0-1]
$\Phi_{lim}^{group}(var)$	= dimensionless limitation or scaling function account for the effect of “lim” on “group” [-]
$k^{var}$	= generic fraction related to “var” [0-1]
$\Theta_{config}^{group}$	= switch to configure selectable model component “config” for “group” [0,1,2,...]
$c, \theta, \gamma \dots$	= coefficient [various units]

### Oxygen

**Table 5: Mass balance and functions related to oxygen cycling.**

<u>Mass balance equations:</u>	
$\frac{dO_2}{dt} = \pm f_{atm}^{O_2} - f_{sed}^{O_2} - \frac{f_{miner}^{DOC}}{\chi_{C:O_2}^{miner}} - \frac{f_{nitrif}}{\chi_{N:O_2}^{nitrif}} + \sum_a^{N_{PHY}} \left( \frac{f_{uptake}^{PHY-Ca}}{\chi_{C:O_2}^{PHY}} \right) - \sum_a^{N_{PHY}} \left( \frac{f_{resp}^{PHY-Ca}}{\chi_{C:O_2}^{PHY}} \right) - \sum_z^{N_{ZOO}} \left( \frac{f_{resp}^{ZOO_z}}{\chi_{C:O_2}^{ZOO}} \right)$	
= ± atmospheric O <sub>2</sub> exchange ± sediment O <sub>2</sub> demand – O <sub>2</sub> consumption by mineralisation of DOC (bacterial respiration) – O <sub>2</sub> consumption by nitrification + O <sub>2</sub> production by photosynthesis – O <sub>2</sub> consumption by phytoplankton respiration – O <sub>2</sub> consumption by zooplankton respiration	
<u>Functions:</u>	
$f_{atm}^{O_2} = \begin{cases} \frac{c_{atm}^{O_2}([O_2]_{atm} - [O_2]_z)}{dz_s} & \text{if } z = z_s \\ 0 & \text{if } z \neq z_s \end{cases}$	atmospheric oxygen exchange
$f_{sed}^{O_2} = F_{max}^{O_2} \frac{O_2}{K_{sed}^{O_2} + O_2} (\theta_{sed}^{O_2})^{T-20} \left( \frac{\widehat{A}_z}{dz_z} \right)$	sediment oxygen demand
where $\widehat{A}_z = A_z^{ben}/A_z$ and $dz_z$ is the thickness of the $z^{\text{th}}$ layer/cell.	

## Silica

**Table 6: Mass balance and functions related to silica cycling.**

<p><u>Balance equations:</u></p> $\frac{dRSi}{dt} = +f_{sed}^{RSi} - \sum_a^{N_{PHY}} f_{uptake}^{PHY-Si_a} + \sum_a^{N_{PHY}} f_{excr}^{PHY-Si_a}$ <p>= + sediment flux – uptake by phytoplankton – excretion by phytoplankton</p> $\frac{dPHY\_Si_a}{dt} = +f_{sett}^{PHY\_Si_a} + \sum_a^{N_{PHY}} f_{uptake}^{PHY-Si_a} - \sum_a^{N_{PHY}} f_{excr}^{PHY-Si_a} - \sum_z^{N_{ZOO}} \left( \frac{f_{assim}^z}{\chi_{C:Si}^{PHY_a}} p_a^z \right)$ <p>= + sedimentation of <math>PHY\_Si_a</math> + uptake by phytoplankton – excretion by phytoplankton – grazing by zooplankton</p>								
<p><u>Functions:</u></p> <table style="width: 100%; border-collapse: collapse;"> <tr> <td style="width: 50%;"> <math>f_{sed}^{RSi} = F_{max}^{RSi} \frac{[O_2]}{K_{sed}^{RSi} + [O_2]} (\theta_{sed}^{RSi})^{T-20} \left( \frac{\widehat{A}_z}{dz_z} \right)</math> </td> <td style="width: 50%;">reactive silica sediment flux</td> </tr> <tr> <td><math>f_{sett}^{PHY\_Si_a} = \frac{\omega_{PHY_a}}{dz_z} [PHY\_Si_a]</math></td> <td>sedimentation of phytoplankton</td> </tr> <tr> <td><math>f_{uptake}^{PHY-Si_a} = f_{uptake}^{PHY-C_a} / \chi_{C:Si}^{PHY_a}</math></td> <td>phytoplankton uptake, linked to photosynthesis rate</td> </tr> <tr> <td><math>f_{excr}^{PHY-Si_a} = \frac{R_{resp}^{PHY_a} (\theta_{resp}^{PHY_a})^{T-20}}{\chi_{C:Si}^{PHY_a}} [PHY\_Si_a]</math></td> <td>excretion / loss of diatom frustules</td> </tr> </table>	$f_{sed}^{RSi} = F_{max}^{RSi} \frac{[O_2]}{K_{sed}^{RSi} + [O_2]} (\theta_{sed}^{RSi})^{T-20} \left( \frac{\widehat{A}_z}{dz_z} \right)$	reactive silica sediment flux	$f_{sett}^{PHY\_Si_a} = \frac{\omega_{PHY_a}}{dz_z} [PHY\_Si_a]$	sedimentation of phytoplankton	$f_{uptake}^{PHY-Si_a} = f_{uptake}^{PHY-C_a} / \chi_{C:Si}^{PHY_a}$	phytoplankton uptake, linked to photosynthesis rate	$f_{excr}^{PHY-Si_a} = \frac{R_{resp}^{PHY_a} (\theta_{resp}^{PHY_a})^{T-20}}{\chi_{C:Si}^{PHY_a}} [PHY\_Si_a]$	excretion / loss of diatom frustules
$f_{sed}^{RSi} = F_{max}^{RSi} \frac{[O_2]}{K_{sed}^{RSi} + [O_2]} (\theta_{sed}^{RSi})^{T-20} \left( \frac{\widehat{A}_z}{dz_z} \right)$	reactive silica sediment flux							
$f_{sett}^{PHY\_Si_a} = \frac{\omega_{PHY_a}}{dz_z} [PHY\_Si_a]$	sedimentation of phytoplankton							
$f_{uptake}^{PHY-Si_a} = f_{uptake}^{PHY-C_a} / \chi_{C:Si}^{PHY_a}$	phytoplankton uptake, linked to photosynthesis rate							
$f_{excr}^{PHY-Si_a} = \frac{R_{resp}^{PHY_a} (\theta_{resp}^{PHY_a})^{T-20}}{\chi_{C:Si}^{PHY_a}} [PHY\_Si_a]$	excretion / loss of diatom frustules							

## Carbon

**Table 7: Mass balance and functions related to carbon cycling.**

<i>Mass balance equations:</i>	
$\frac{dDOC}{dt} = f_{decom}^{POC} - f_{miner}^{DOC} + f_{sed}^{DOC} + \sum_a^{N_{PHY}} f_{excr}^{PHY-Ca} + \sum_z^{N_{ZOO}} f_{excr}^z$	= POC decomposition – DOC mineralisation + sediment flux + phytoplankton excretion/exudation + zooplankton excretion
$\frac{dPOC}{dt} = -f_{decom}^{POC} - f_{sett}^{POC} + \sum_a^{N_{PHY}} f_{mort}^{PHY-Ci} + \sum_z^{N_{ZOO}} [(1 - k_{assim}^z) f_{assim}^z + (1 - k_{fsed}^z) f_{fecal}^z + f_{mort}^z]$	= – POC hydrolysis and decomposition – POC settling + phytoplankton mortality + zooplankton messy feeding + zooplankton fecal pellet + zooplankton mortality
$\frac{d(PHY-Ca)}{dt} = +f_{uptake}^{PHY-Ca} - f_{excr}^{PHY-Ca} - f_{mort}^{PHY-Ca} - f_{resp}^{PHY-Ca} - f_{sett}^{PHY-Ca} - \sum_z^{N_{ZOO}} f_{assim}^z \times p_a^z$	= + carbon fixation through photosynthesis + excretion/exudation of DOC – mortality – respiration – sedimentation – zooplankton grazing
$\frac{d(ZOO_z)}{dt} = k_{assim}^z \times f_{assim}^z - f_{loss}^z - f_{mort}^z$	= + carbon assimilation via grazing – carbon loss via respiration, excretion of DOC, fecal pellets production – mortality
$TOC = DOC + POC + \sum_a^{N_{PHY}} PHY-Ca + \sum_z^{N_{ZOO}} ZOO_z$	
<i>Functions:</i>	
$f_{sed}^{DOC} = F_{max}^{DOC} \frac{K_{sed}^{DOC}}{K_{sed}^{DOC} + [DOC]} (\theta_{sed}^{DOC})^{T-20} \left( \frac{A_z}{dz_z} \right)$	DOC sediment flux
$f_{sett}^{POC} = \frac{\omega_{POC}}{dz_z} [POC]$	sedimentation of particulate organic carbon
$f_{decom}^{POC} = R_{decom}^{POC} \frac{[O_2]}{K_{miner}+[O_2]} (\theta_{decom})^{T-20} [POC]$	hydrolysis/decomposition of POC
$f_{miner}^{DOC} = R_{miner}^{DOC} \frac{[O_2]}{K_{miner}+[O_2]} (\theta_{miner})^{T-20} [DOC]$	mineralisation of DOC
$f_{sett}^{PHY-Ca} = \frac{\omega_{PHYa}}{dz_z} [PHY-Ca]$	sedimentation of phytoplankton
$f_{uptake}^{PHY-Ca} = R_{growth}^{PHYa} \Phi_{tem}^{PHYa}(T) \min\{\Phi_{light}^{PHYa}(I), \Phi_N^{PHYa}(NO_3, NH_4), \Phi_p^{PHYa}(PO_4), \Phi_{Si}^{PHYa}(RSi)\} [PHY-Ca]$	photosynthesis
$f_{excr}^{PHY-Ca} = (1 - k_{fres}^{PHYa}) k_{fdom}^{PHYa} R_{resp}^{PHYa} (\theta_{resp}^{PHYa})^{T-20} [PHY-Ca]$	excretion of dissolved organic carbon
$f_{mort}^{PHY-Ca} = (1 - k_{fres}^{PHYa}) (1 - k_{fdom}^{PHYa}) R_{resp}^{PHYa} (\theta_{resp}^{PHYa})^{T-20} [PHY-Ca]$	mortality to organic carbon
$f_{excr}^{PHY-Ca} = k_{fres}^{PHYa} R_{resp}^{PHYa} (\theta_{resp}^{PHYa})^{T-20} [PHY-Ca]$	phytoplankton respiration
$f_{assim}^z = R_{grz}^{ZOO} \Phi_{tem}^z(T) [ZOO]$	zooplankton assimilation
$f_{loss}^z = R_{loss}^{ZOO} (\theta_{loss}^z)^{T-20} [ZOO]$	zooplankton loss
$f_{excr}^z = k_{excr}^z \times f_{loss}^z$	zooplankton excretion
$f_{fecal}^z = k_{fecal}^z \times f_{loss}^z$	zooplankton fecal pellets
$f_{mort}^z = R_{mort}^z \Phi_{sal}^z(S) \times (\theta_{loss}^z)^{T-20} [ZOO]$	zooplankton mortality

## Nitrogen

**Table 8: Mass balance and functions related to nitrogen cycling.**

<i>Mass balance equations:</i>	
$\frac{dNH_4}{dt} = +f_{sed}^{NH_4} + f_{miner}^{DON} - f_{nitrif}^{NH_4} - \sum_i^{NPHY} [p_{NH_4}^a \times f_{uptake}^{PHY-Na}]$	= + sediment flux + mineralisation of PON – nitrification – phytoplankton NH <sub>4</sub> uptake
$\frac{dNO_3}{dt} = -f_{sed}^{NO_3} + f_{nitrif}^{NH_4} - f_{denit}^{NO_3} - \sum_a^{NPHY} [p_{NO_3}^a \times f_{uptake}^{PHY-Na}]$	= + sediment flux + nitrification – denitrification – phytoplankton NO <sub>3</sub> uptake
$\frac{dDON}{dt} = +f_{decom}^{PON} + f_{sed}^{DON} - f_{miner}^{DON} + \sum_a^{NPHY} f_{excr}^{PHY-Na} + \sum_z^{NZOO} \frac{f_{excr}^z}{\chi_{C:N}^z}$	= + PON decomposition/hydrolysis + sediment flux – DON mineralisation + phytoplankton excretion + zooplankton excretion
$\frac{dPON}{dt} = -f_{decom}^{PON} - f_{sett}^{PON} + \sum_i^{NPHY} f_{mort}^{PHY-Na} + \sum_z^{NZOO} [(1 - k_{assim}^z) f_{assim}^z + (1 - k_{fsed}^z) f_{fecal}^z + f_{mort}^z] \frac{1}{\chi_{C:N}^z}$	= – PON decomposition/hydrolysis – PON settling + phytoplankton mortality + zooplankton messy feeding + zooplankton fecal pellet + zooplankton mortality
$\frac{d(PHY\_Na)}{dt} = +f_{uptake}^{PHY-Na} - f_{excr}^{PHY-Na} - f_{mort}^{PHY-Na} - f_{sett}^{PHY-Na} - \sum_z^{NZOO} \left( f_{assim}^z \times p_a^z \times \frac{PHY\_P_a}{PHY\_C_a} \right)$	= + N uptake + excretion of DON – mortality– sedimentation – zooplankton grazing
$TN = NO_3 + NH_4 + DON + PON + \sum_a^{NPHY} PHY\_Na \sum_z^{NZOO} \frac{ZOO_z}{\chi_{C:N}^z}$	
<i>Functions:</i>	
$f_{sed}^{NH_4} = F_{max}^{NH_4} \frac{K_{sed}^{NH_4}}{K_{sed}^{NH_4} + [O_2]} (\theta_{sed}^{NH_4})^{T-20} \left( \frac{\widehat{A}_z}{dz_z} \right)$	ammonium sediment flux
$f_{sed}^{NO_3} = F_{max}^{NO_3} \frac{[O_2]}{K_{sed}^{NO_3} + [O_2]} (\theta_{sed}^{NO_3})^{T-20} \left( \frac{\widehat{A}_z}{dz_z} \right)$	nitrate sediment flux
$f_{sed}^{DON} = F_{max}^{DON} \frac{K_{sed}^{DON}}{K_{sed}^{DON} + [DON]} (\theta_{sed}^{DON})^{T-20} \left( \frac{\widehat{A}_z}{dz_z} \right)$	DON sediment flux
$f_{sett}^{PON} = \frac{\omega_{PON}}{dz_z} [PON]$	sedimentation of particulate organic nitrogen
$f_{sett}^{PHY-Ni} = \frac{\omega_{PHY_i}}{dz_z} [PHY\_Na]$	sedimentation of phytoplankton
$f_{decom}^{PON} = R_{decom}^{PON} \frac{[O_2]}{K_{miner}^{PON} + [O_2]} (\theta_{decom}^{PON})^{T-20} [PON]$	hydrolysis/decomposition of PON
$f_{miner}^{DON} = R_{miner}^{DON} \frac{[O_2]}{K_{miner}^{DON} + [O_2]} (\theta_{miner}^{DON})^{T-20} [DON]$	mineralisation of DON
$f_{nitrif}^{NH_4} = R_{nitrif}^{NH_4} \frac{[O_2]}{K_{nitrif}^{NH_4} + [O_2]} (\theta_{nitrif}^{NH_4})^{T-20} [NH_4]$	nitrification

$f_{denit}^{NO_3} = R_{denit} \frac{K_{denit}}{K_{denit} + [O_2]} (\theta_{denit})^{T-20} [NO_3]$	denitrification
$f_{uptake}^{PHY\_Na} = \begin{cases} f_{uptake}^{PHY\_Ca} / \chi_{C:N}^{PHY_a} & \text{if } \Theta_{NUptake}^{PHY_a} = 1 \text{ (STATIC)} \\ R_{NUptake}^{PHY_a} \Phi_{tem}^{PHY_a}(T) \left\{ \Phi_N^{PHY_a}([NO_3], [NH_4]) \frac{\left( \frac{[PHY\_Na]}{[PHY\_Ca]} - \chi_{NMIN}^{PHY_a} \right)}{\left( \chi_{NMAX}^{PHY_a} - \chi_{NMIN}^{PHY_a} \right)} \right\} [PHY\_Na] & \text{if } \Theta_{NUptake}^{PHY_a} = 2 \text{ (DROOP)} \end{cases}$	nitrogen uptake by nitrogen
$f_{excr}^{PHY\_Na} = \frac{k_{fdom}^{PHY_a}}{\chi_{C:N}^{PHY_a}} R_{resp}^{PHY_a} (\theta_{resp}^{PHY_a})^{T-20} [PHY\_Na]$	nitrogen excretion from phytoplankton
$f_{mort}^{PHY\_Na} = \frac{(1 - k_{fdom}^{PHY_a})}{\chi_{C:N}^{PHY_a}} R_{resp}^{PHY_a} (\theta_{resp}^{PHY_a})^{T-20} [PHY\_Na]$	nitrogen component of phytoplankton mortality
$p_{NH4}^{PHY_a} = \frac{[NO_3][NH_4]}{([NH_4] + K_N^{PHY_a})([NO_3] + K_N^{PHY_a})} \frac{[NH_4] K_N^{PHY_a}}{([NH_4] + [NO_3])([NO_3] + K_N^{PHY_a})}$	preference of phytoplankton for NH <sub>4</sub>
$p_{NO3}^{PHY_a} = 1 - p_{NH4}^{PHY_a}$	preference of phytoplankton for NO <sub>3</sub>

## Phosphorus

**Table 9: Mass balance and functions related to phosphorus cycling.**

<i>Mass balance equations:</i>	
$\frac{dPO_4}{dt} = +f_{sed}^{PO_4} + f_{miner}^{DOP} \pm f_{ads}^{PO_4} - \sum_a^{N_{PHY}} [f_{uptake}^{PHY-Pa}]$	= + sediment flux + mineralisation of DOP ± adsorption/desorption – phytoplankton PO <sub>4</sub> uptake
$\frac{dPO_4^{ads}}{dt} = \pm f_{ads}^{PO_4} - f_{sett}^{PO_4^{ads}}$	= ± adsorption/desorption – sedimentation
$\frac{dPOP}{dt} = -f_{decom}^{POP} - f_{sett}^{POP} + \sum_a^{N_{PHY}} f_{mort}^{PHY-Pa} + \sum_z^{N_{ZOO}} [(1 - k_{assim}^z) f_{assim}^z + (1 - k_{fsed}^z) f_{fecal}^z + f_{mort}^z] \frac{1}{\chi_{C:P}^z}$	= – POP decomposition/hydrolysis – POP settling + phytoplankton mortality + zooplankton messy feeding + zooplankton fecal pellet + zooplankton mortality
$\frac{dDOP}{dt} = f_{decom}^{POP} - f_{miner}^{DOP} + f_{sed}^{DOP} + \sum_a^{N_{PHY}} f_{excr}^{PHY-Pa} + \sum_z^{N_{ZOO}} 1/\chi_{C:P}^z f_{excr}^z$	= POP mineralisation – POP settling + phytoplankton excretion + zooplankton excretion
$\frac{d(PHY\_P_i)}{dt} = +f_{uptake}^{PHY\_P_i} - f_{excr}^{PHY\_P_i} - f_{mort}^{PHY\_P_i} - f_{sett}^{PHY\_P_i} - \sum_z^{N_{ZOO}} (f_{assim}^z \times p_a^z \times \frac{PHY\_P_a}{PHY\_C_a})$	= + P uptake + excretion of DOP – mortality – sedimentation – zooplankton grazing
$TP = PO_4 + DOP + POP + \sum_a^{N_{PHY}} PHY\_P_a + \sum_z^{N_{ZOO}} \frac{ZOO_z}{\chi_{C:P}^z}$	
<i>Functions:</i>	
$f_{sed}^{PO_4} = F_{max}^{PO_4} \frac{K_{sed}^{PO_4}}{K_{sed}^{PO_4} + [O_2]} (\theta_{sed}^{PO_4})^{T-20} \left( \frac{\widehat{A}_z}{dz_z} \right)$	phosphate sediment flux
$f_{sed}^{DOP} = F_{max}^{DOP} \frac{K_{sed}^{DOP}}{K_{sed}^{DOP} + [DOP]} (\theta_{sed}^{DOP})^{T-20} \left( \frac{\widehat{A}_z}{dz_z} \right)$	dissolved organic phosphorus sediment flux
$f_{sett}^{POP} = \frac{\omega_{POP}}{dz_z} [POP]$	sedimentation of particulate organic phosphorus
$f_{sett}^{PHY\_Pa} = \frac{\omega_{PHY\_Pa}}{dz_z} [PHY\_Pa]$	sedimentation of phytoplankton
$f_{uptake}^{PHY\_Pa} = \begin{cases} f_{uptake}^{PHY\_C_a} / \chi_{C:P}^{PHY\_a} & \text{if } \Theta_{PUptake}^{PHY\_a} = 1 \text{ (STATIC)} \\ R_{PUptake}^{PHY\_a} \Phi_{tem}^{PHY\_a}(T) \left\{ \Phi_P^{PHY\_a}([PO_4]) \frac{(\frac{[PHY\_Pa]}{[PHY\_C_a]} - \chi_{PMIN}^{PHY\_a})}{(\chi_{PMAx}^{PHY\_a} - \chi_{PMIN}^{PHY\_a})} \right\} [PHY\_Pa] & \text{if } \Theta_{PUptake}^{PHY\_a} = 2 \text{ (DROOP)} \end{cases}$	phosphorus uptake by phytoplankton
$f_{excr}^{PHY\_Pa} = \frac{k_{fdom}^{PHY\_a}}{\chi_{C:P}^{PHY\_a}} R_{resp}^{PHY\_a} (\theta_{resp}^{PHY\_a})^{T-20} [PHY\_Pa]$	phosphorus excretion from phytoplankton

$$f_{mort}^{PHY\_P_i} = \frac{(1-k_f^{PHYa})}{\chi_{C,P}^{PHYa}} R_{resp}^{PHYa} (\theta_{resp}^{PHYa})^{T-20} [PHY\_P_a] \quad \text{phosphorus contribution from phytoplankton mortality}$$

$$f_{sett}^{PO_4^{ads}} = \frac{\omega_{SS}}{dz_z} [PO_4^{ads}] \quad \text{sedimentation of adsorbed phosphorus}$$

$$f_{ads}^{PO_4} = \left[ \Phi_{ads}^{PO_4} ([PO_4 + PO_4^{ads}]^{t+1}, SS, pH) \times [PO_4 + PO_4^{ads}]^{t+1} - PO_4^{ads*} \right] \frac{1}{\Delta t} \quad \text{adsorption/desorption 'rate' of phosphorus}$$

$$\Phi_{ads}^{PO_4}(IP, SS, pH) = \frac{1}{2IP} \left[ \left( IP + \frac{1}{c_{ads}^r} + c_{ads}^{max} \Phi_{ads}^{pH}(pH) SS \right) - \sqrt{\left( IP + \frac{1}{c_{ads}^r} + c_{ads}^{max} \Phi_{ads}^{pH}(pH) SS \right)^2 + \frac{4c_{ads}^{max} \Phi_{ads}^{pH}(pH)}{c_{ads}^r} SS} \right]$$

adsorped fraction of total available inorganic phosphorus (IP)

## Parameter summary

**Table 10: Summary of sediment parameter descriptions, units and typical values.**

Symbol	Description	Units	Default value	Comment
$F_{max}^{O_2}$	maximum flux of oxygen across the sediment water interface into the sediment	mmol O <sub>2</sub> /m <sup>2</sup> /d	48.0	Lake: 6 – 38 <sup>A</sup> River: 9.4 – 20.3 <sup>B</sup> Estuary: 48 <sup>C</sup> ; 79 <sup>D</sup> ; ~50 <sup>E</sup>
$K_{sed}^{O_2}$	half saturation constant for oxygen dependence of sediment oxygen flux	mmol O <sub>2</sub> /m <sup>3</sup>	150	Lake: 15.6 <sup>A</sup> Estuary: 150 <sup>C</sup> ; ~50 <sup>F</sup>
$\theta_{sed}^{O_2}$	temperature multiplier for temperature dependence of sediment oxygen flux	-	= $\theta_{sed}$ = 1.08	1.04 – 1.10 <sup>A</sup>
$F_{max}^{RSi}$	maximum flux of silica across the sediment water interface	mmol Si/m <sup>2</sup> /d	4	Lake: 0.6 <sup>A</sup> Estuary: 4 – 40 <sup>E</sup>
$K_{sed}^{RSi}$	half saturation constant for oxygen dependence of sediment silica flux	mmol Si/m <sup>3</sup>	150	estimated
$\theta_{sed}^{RSi}$	temperature multiplier for temperature dependence of sediment silica flux	-	= $\theta_{sed}$ = 1.08	1.04 – 1.10 <sup>A</sup>
$F_{max}^{PO_4}$	maximum flux of phosphate across the sediment water interface	mmol P/m <sup>2</sup> /d	0.2	Lake: 0.080 – 0.125 <sup>A</sup> River: 0.0 – 0.10 <sup>B</sup> Estuary: 0.3 – 4 <sup>E</sup>
$K_{sed}^{PO_4}$	half saturation constant for oxygen dependence of sediment phosphate flux	mmol O <sub>2</sub> /m <sup>3</sup>	20	Lake: 15.6 <sup>A,j</sup> Estuary: >200 <sup>F</sup>
$\theta_{sed}^{PO_4}$	temperature multiplier for temperature dependence of sediment phosphate flux	-	= $\theta_{sed}$ = 1.08	1.04 – 1.10 <sup>A</sup>
$F_{max}^{DOP}$	maximum flux of dissolved organic phosphorus across the sediment water interface	mmol P/m <sup>2</sup> /d	0.05	Lake: 0.03 <sup>A</sup> River: 0.05 – 0.10 <sup>B</sup>
$K_{sed}^{DOP}$	half saturation constant for oxygen dependence of sediment dissolved organic phosphorus flux	mmol O <sub>2</sub> /m <sup>3</sup>	150	estimated
$\theta_{sed}^{DOP}$	temperature multiplier for temperature dependence of sediment dissolved organic phosphorus flux	-	= $\theta_{sed}$ = 1.08	1.04 – 1.10 <sup>A</sup>
$F_{max}^{NH_4}$	maximum flux of ammonium across the sediment water interface	mmol N/m <sup>2</sup> /d	30.0	Lake: 1.35 – 6.42 <sup>A</sup> River: 4.3 – 12.8 <sup>B</sup> Estuary: 30 <sup>C</sup> ; 5 – 25 <sup>E</sup>
$K_{sed}^{NH_4}$	half saturation constant for oxygen dependence of sediment ammonium flux	mmol N/m <sup>3</sup>	31.25	Lake: 1.56 – 15.6 <sup>A</sup> Estuary: 31.25 <sup>C</sup>
$\theta_{sed}^{NH_4}$	temperature multiplier for temperature dependence of sediment ammonium flux	-	1.08	1.04 – 1.10 <sup>A</sup>
$F_{max}^{NO_3}$	maximum flux of nitrate across the sediment water interface	mmol N/m <sup>2</sup> /d	5.2	Lake: -21.4 – -7.14 <sup>A</sup> River: 4.3 – 12.8 <sup>B</sup> Estuary: 5.2 <sup>C</sup> ; -7.2 – 7.1 <sup>E</sup>
$K_{sed}^{NO_3}$	half saturation constant for oxygen dependence of sediment nitrate flux	mmol O <sub>2</sub> /m <sup>3</sup>	100.0	Lake: 2.14 – 15.6 <sup>A</sup> Estuary: 100 <sup>C</sup>
$\theta_{sed}^{NO_3}$	temperature multiplier for temperature dependence of sediment nitrate flux	-	= $\theta_{sed}$ = 1.08	1.04 – 1.10 <sup>A</sup>
$F_{max}^{DON}$	maximum flux of dissolved organic nitrogen across the sediment water interface	mmol N/m <sup>2</sup> /d	5.2	Lake: 0.07 – 0.57 <sup>A</sup> River: 1.28 – 2.20 <sup>B</sup>
$K_{sed}^{DON}$	half saturation constant for oxygen dependence of sediment dissolved organic nitrogen flux	mmol N/m <sup>3</sup>	100.0	estimated
$\theta_{sed}^{DON}$	temperature multiplier for temperature dependence of sediment dissolved organic nitrogen flux	-	= $\theta_{sed}$ = 1.08	1.04 – 1.10 <sup>A</sup>

<sup>A</sup> Converted from data on oligotrophic lakes (Romero et al. 2004) to eutrophic lakes (Gal et al. 2009), and justifications therein .

<sup>B</sup> Based on Hipsey et al. (2010) ELCOM-CAEDYM model of the lower Murray River); estimated from data from Justin Brookes.

<sup>C</sup> Based on Bruce et al. (*submitted*) GETM-FABM-AED application on the Yarra Estuary (Victoria); estimated from data from Perran Cook.

<sup>D</sup> Net flux measured during eddy correlation experiment in the Upper Swan Estuary (Kilmister et al., 2011); varied in the range 20 – 150 mmol O<sub>2</sub>/m<sup>2</sup>/d with a background concentration of 260 mmol O<sub>2</sub>/m<sup>3</sup>, therefore  $F_{max}^{O_2} \approx 50/(260/(260+150)) = 79$  mmol O<sub>2</sub>/m<sup>2</sup>/d.

<sup>E</sup> Based on benthic chamber studies showing an average net flux of 50 mmol O<sub>2</sub>/m<sup>2</sup>/d the Upper Swan estuary (Smith et al 2007).

<sup>F</sup> Based on Smith et al (2007) assessment of data from the Upper Swan estuary, limitation at low oxygen concentrations is not observed

**Table 11: Summary of water column biogeochemical parameter descriptions, units and typical values.**

Symbol	Description	Units	Assigned value	Comment
$k_{atm}^{O_2}$	oxygen transfer coefficient	m/s	calculated	<i>Wanninkhof (1992)</i>
$[O_2]_{atm}$	atmospheric oxygen concentration	mmol O <sub>2</sub> /m <sup>3</sup>	calculated	<i>Riley and Skirrow (1975)</i>
$\chi_{C:O_2}^{miner}, \chi_{C:O_2}^{PHY}$	Stoichiometric conversion of C to O <sub>2</sub>	mmol C/mmol O <sub>2</sub>		12/32
$\chi_{N:O_2}^{nitrif}$	Stoichiometric conversion of N to O <sub>2</sub>	mmol N/mmol O <sub>2</sub>		14/32
$R_{nitrif}$	maximum rate of nitrification	/d	0.5	<i>Lake: 0.03 – 0.05<sup>A</sup>; 0.037<sup>G</sup></i> <i>Estuary: 0.5<sup>C</sup></i>
$K_{nitrif}$	half saturation constant for oxygen dependence of nitrification rate	mmol O <sub>2</sub> /m <sup>3</sup>	78.1	<i>Lake: 62.5 – 93.7<sup>A</sup></i> <i>Estuary: 78.1<sup>C</sup></i>
$\theta_{nitrif}$	temperature multiplier for temperature dependence of nitrification rate	-	1.08	<i>Lake: 1.08<sup>A</sup>; 1.03<sup>G</sup></i> <i>Estuary: 1.08<sup>C</sup></i>
$R_{denit}$	maximum rate of denitrification	/d	0.5	<i>Lake: 0.01 – 0.04<sup>A</sup></i> <i>Estuary: 0.5<sup>C</sup></i>
$K_{denit}$	half saturation constant for oxygen dependence of denitrification	mmol O <sub>2</sub> /m <sup>3</sup>	21.8	<i>Lake: 12.5 – 15.6<sup>A</sup></i> <i>Estuary: 21.8<sup>C</sup></i>
$\theta_{denit}$	temperature multiplier for temperature dependence of denitrification	-	1.08	<i>Lake: 1.05<sup>A</sup></i> <i>Estuary: 1.08<sup>C</sup></i>
$R_{decom}^{PON}$	maximum rate of decomposition of particulate organic nitrogen	/d	0.5	<i>Lake: 0.005 – 0.01<sup>A</sup>; 0.03<sup>G</sup></i> <i>Estuary: 0.5<sup>C</sup></i>
$K_{decom}^{PON}$	half saturation constant for oxygen dependence of mineralisation rate	mmol O <sub>2</sub> /m <sup>3</sup>	31.25	<i>Lake: 47 – 78<sup>A</sup></i> <i>Estuary: 31.25<sup>C</sup></i>
$\theta_{decom}^{PON}$	temperature multiplier for temperature dependence of mineralisation rate	-	= $\theta_{OM} = 1.08$	<i>Lake: 1.08<sup>A</sup></i> <i>Estuary: 1.08<sup>C</sup></i>
$R_{miner}^{DON}$	maximum rate of mineralisation of dissolved organic nitrogen	/d	0.5	<i>Lake: 0.003 – 0.05<sup>A</sup></i> <i>Estuary: 0.001 – 0.028<sup>H</sup></i>
$K_{decom}^{DON}$	half saturation constant for oxygen dependence of mineralisation rate	mmol O <sub>2</sub> /m <sup>3</sup>	31.25	<i>Lake: 47 – 78<sup>A</sup></i>
$\theta_{miner}^{DON}$	temperature multiplier for temperature dependence of mineralisation rate	-	= $\theta_{OM} = 1.08$	1.04 – 1.10 <sup>A</sup>
$\omega_{PON}$	settling rate of particulate organic matter	m/d	= $\omega_{OM} = -1.0$	<i>Estuary: -1.0<sup>C</sup></i>
$R_{decom}^{POC}$	maximum rate of decomposition of particulate organic carbon	/d	0.5	<i>Lake: 0.01 – 0.07<sup>A</sup>; 0.008<sup>G</sup></i>
$K_{decom}^{POC}$	half saturation constant for oxygen dependence of mineralisation rate	mmol O <sub>2</sub> /m <sup>3</sup>	31.25	<i>Lake: 47 – 78<sup>A</sup></i>
$\theta_{decom}^{POC}$	temperature multiplier for temperature dependence of mineralisation rate	-	= $\theta_{OM} = 1.08$	1.04 – 1.10 <sup>A</sup>
$R_{miner}^{DOC}$	maximum rate of mineralisation of dissolved organic carbon	/d	0.5	<i>Lake: 0.003 – 0.05<sup>A</sup></i> <i>Estuary: 0.001 – 0.006<sup>H</sup></i>
$K_{decom}^{DOC}$	half saturation constant for oxygen dependence of mineralisation rate	mmol O <sub>2</sub> /m <sup>3</sup>	31.25	<i>Lake: 47 – 78<sup>A</sup></i>
$\theta_{miner}^{DOC}$	temperature multiplier for temperature dependence of mineralisation rate	-	= $\theta_{OM} = 1.08$	1.04 – 1.10 <sup>A</sup>
$\omega_{POC}$	settling rate of particulate organic matter	m/day	= $\omega_{OM} = -1.0$	
$R_{decom}^{POP}$	maximum rate of decomposition of particulate organic phosphorus	/d	0.5	<i>Lake: 0.01 – 0.03<sup>A</sup>; 0.099<sup>G</sup></i>
$K_{decom}^{POP}$	half saturation constant for oxygen dependence of mineralisation rate	mmol O <sub>2</sub> /m <sup>3</sup>	31.25	<i>Lake: 47 – 78<sup>A</sup></i>
$\theta_{decom}^{POP}$	temperature multiplier for temperature dependence of mineralisation rate	-	= $\theta_{OM} = 1.08$	1.04 – 1.10 <sup>A</sup>
$R_{miner}^{DOP}$	maximum rate of mineralisation of dissolved organic phosphorus	/d	0.5	<i>Lake: 0.01 – 0.05<sup>A</sup></i>

$K_{decom}^{DOP}$	half saturation constant for oxygen dependence of mineralisation rate	mmol O <sub>2</sub> /m <sup>3</sup>	31.25	<i>Lake: 47 – 78<sup>A</sup></i>
$\theta_{miner}^{DOP}$	temperature multiplier for temperature dependence of mineralisation rate	-	= $\theta_{OM} = 1.08$	1.04 – 1.10 <sup>A</sup>
$\omega_{POP}$	settling rate of particulate organic matter	m/d	= $\omega_{OM} = -1.0$	
$\Phi_{ads}^{pH}(pH)$	Function characterizing pH effect on	-	calculated	-0.0088(pH) <sup>2</sup> + 0.0347(pH) + 0.9768 <sup>I</sup>
$c_{ads}^r$	ratio of adsorption and desorption rate coefficients	l/mg		<i>Lake: 0.7<sup>J</sup></i>
$c_{ads}^{max}$	maximum adsorption capacity of SS	mmol P/mg SS		<i>Lake: 0.00016<sup>J</sup></i>

- A Converted from data on oligotrophic lakes (Romero et al. 2004) to eutrophic lakes (Gal et al. 2009), and justifications therein .  
 C Based on Bruce et al. (*submitted*) GETM-FABM-AED application on the Yarra Estuary (Victoria); estimated from data from Perran Cook.  
 G Based on Schladow & Hamilton (1997) for Prospect Reservoir  
 H Based on incubations by Petrone et al. (2009) for Swan Estuary (Western Australia)  
 I Based on regression of data from Salmon et al. (*in prep*) based on data review from 6 papers  
 J Based on model of Chao et al. (2010).

**Table 12: Summary of phytoplankton parameter descriptions, units and typical values.**

parameter	description	units	Group #1	Group #2	Group #3	Comment
$R_{growth}^{PHY}$	phytoplankton growth rate at 20C	/d	3.0	0.9	1.0	Various
$I_K$	light ½ saturation constant for algal limitation	μE m <sup>-2</sup> s <sup>-1</sup>	60	80	130	Romero et al. (2004)
$I_s$	saturating light intensity	μE m <sup>-2</sup> s <sup>-1</sup>	150	150	150	Schladow & Hamilton (1997)
$\theta_{growth}^{PHY}$	Arrhenius temperature scaling for growth	-	1.06	1.06	1.06	Kruger and Ellor (1978), Coles and Jones (2000), Schladow & Hamilton (1997)
$T_{std}$	standard temperature	C	20	20	20	Griffin et al. (2001)
$T_{opt}$	optimum temperature	C	25	27	28	Griffin et al. (2001)
$T_{max}$	maximum temperature	C	32	33	35	Griffin et al. (2001)
$R_{resp}^{PHY}$	phytoplankton respiration rate at 20C	/d	0.085	0.085	0.085	Schladow & Hamilton (1997)
$k_{fres}^{PHY}$	fraction of metabolic loss that is respiration	-	0.25	0.25	0.25	Gal et al. 2009
$k_{fdom}^{PHY}$	fraction of metabolic loss that is DOM	-	0.2	0.2	0.2	Gal et al. 2009
$\theta_{resp}^{PHY}$	Arrhenius temperature scaling for respiration	-	1.12	1.05	1.05	Gal et al. 2009
$K_N$	half-saturation concentration of nitrogen	mmol N /m <sup>3</sup>	3.5	2.7	1.0	Gal et al. 2009
$R_{NUptake}^{PHY}$	maximum nitrogen uptake rate	mmol N /m <sup>3</sup> /d				
$\chi_{NMIN}^{PHY}$	minimum internal nitrogen concentration	mmol N / mmol C				
$\chi_{NMAX}^{PHY}$	maximum internal nitrogen concentration	mmol N / mmol C				
$K_P$	half-saturation concentration of phosphorus	mmol P /m <sup>3</sup>	0.15	0.07	0.05	Gal et al. 2009
$R_{NUptake}^{PHY}$	maximum phosphorus uptake rate	mmol P /m <sup>3</sup> /d				
$\chi_{PMIN}^{PHY}$	minimum internal phosphorus concentration	mmol P / mmol C				
$\chi_{PMAX}^{PHY}$	maximum internal phosphorus concentration	mmol P / mmol C				
$K_{Si}$	half-saturation concentration of silica	mmol Si /m <sup>3</sup>	2.5	-	-	Romero et al. 2004
$\chi_{C:Si}^{PHYa}$	internal silicate concentration	mmol Si / mmol C		-	-	
$\omega_{PHY}$	phytoplankton sedimentation rate	m/d	-0.86	-0.01	-0.02	Gal et al. 2009; Romero et al. 2004

Note that in collaboration with the Aquatic Ecological Modelling Network (AEMON), we are developing a database of species parameters which may be referred to search for specific parameters for a given species, or to see typical values for functional groups used in other modelling studies:

<https://sites.google.com/site/aquaticmodelling/>

Click on *Resources* and then follow the link to “*Parameter database*”

**Table 13: Summary of zooplankton parameter descriptions, units and typical values.**

parameter	description	units	Group #1	
$\varepsilon_{min}^z$	Minimum zooplankton concentration	mmol C/m <sup>3</sup>	0.1	
$R_{grz}^z$	Zooplankton grazing rate	/day	1.5	
$k_{assim}^z$	Assimilation efficiency for zooplankton grazing	-	0.9	
$K_{grz}^z$	Half saturation constant for zooplankton grazing	-	40	
$\theta_{grz}^z$	Temperature multiplier for zooplankton grazing	-	1.08	
$T_{std}^z$	Standard temperature for zooplankton grazing	°C	20.0	
$T_{opt}^z$	Optimum temperature for zooplankton grazing	°C	22.0	
$T_{max}^z$	Maximum temperature for zooplankton grazing	°C	30.0	
$p_z^z$	Preference factor of zooplankton grazing on phytoplankton	-	0.7	
$p_{PHY\_a}^z$	Preference factor of zooplankton grazing on zooplankton	-	0.0	
$p_{POM}^z$	Preference factor of zooplankton grazing on particulate organic matter	-	0.3	
$p_b^z$	Preference factor of zooplankton grazing on bacteria	-	0.0	
$\varepsilon_{grz}^z$	Concentration of prey at which grazing by zooplankton is limited	mmol C/m <sup>3</sup>	10.0	
$R_{loss}^z$	Respiration rate coefficient	/day	0.1	
$R_{mort}^z$	Mortality rate coefficient	/day	0.01	
$k_{fecal}^z$	Fecal pellet fraction of loss rate	-	0.2	
$k_{excr}^z$	Excretion fraction of loss rate	-	0.7	
$k_{fsed}^z$	Fraction of fecal pellets that sink directly to sediments (hard fraction)	-	0.15	
$\theta_{loss}^z$	Temperature multiplier for zooplankton loss	-	1.08	
$\chi_{C:N}^z$	Ratio of internal nitrogen to carbon	mmol N / mmol C	0.2	
$\chi_{C:P}^z$	Ratio of internal phosphorus to carbon	mmol P / mmol C	0.01	
$\theta_{sal}^z$	Type of salinity limitation function		1	
$S_{max}^z$	Maximum or optimal salinity	psu	0.0	
$S_{min}^z$	Minimum salinity	psu	35.0	
$S_{int}^z$	Salinity intercept, for S=0	-	10.0	
$\theta_{oxy}^z$	Simulate oxygen limitation		1	
$\varepsilon_{oxy}^z$	Minimum concentration of dissolved oxygen at which zooplankton can survive	mmol O <sub>2</sub> /m <sup>3</sup>	0.05	

# GLM-FABM-AED Setup

## Overview

Here a description of the structure of a GLM-FABM setup is described with particular reference to setting up the AED modules of FABM, however the general approach will be relevant for all FABM models. The model takes two main configuration files, one each for GLM and FABM, and several time-series and specialist parameter database files (Figure 5).

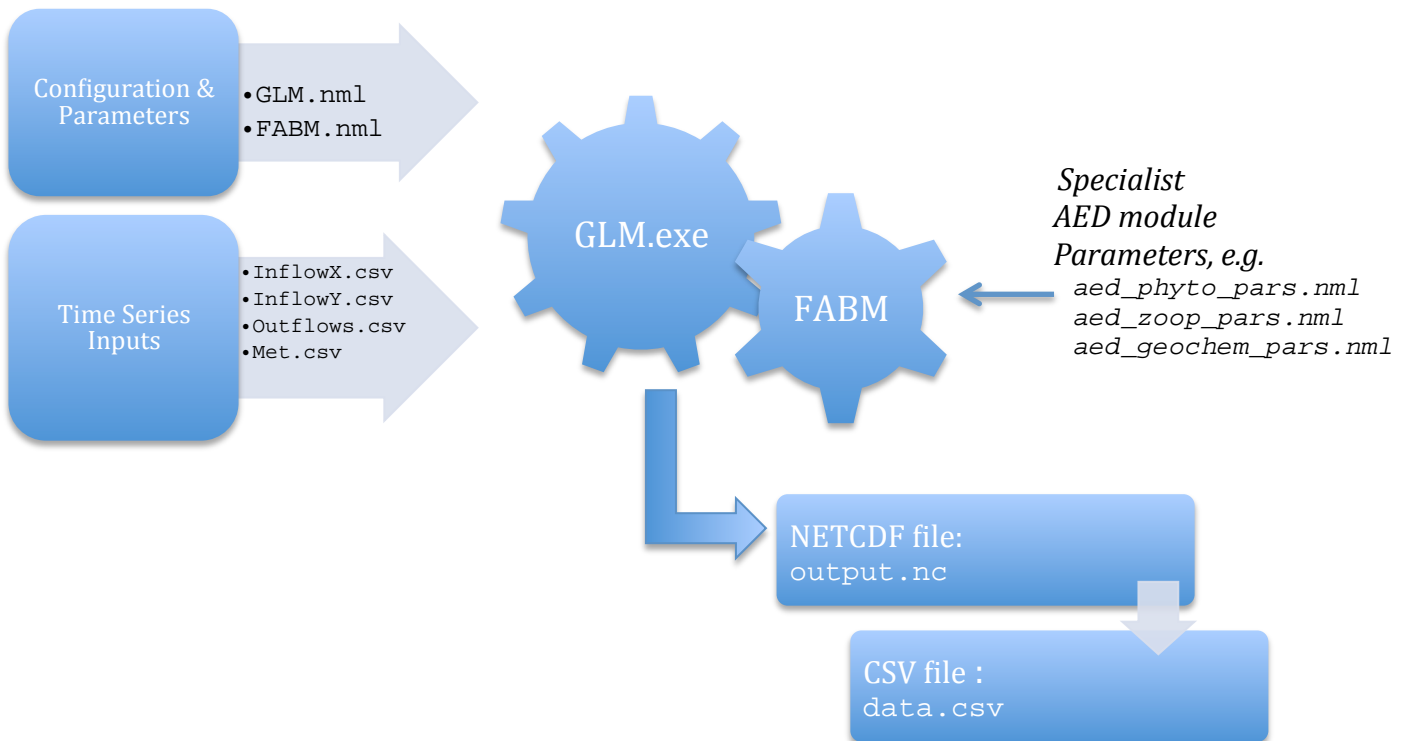


Figure 5: Flow diagram showing the files required for operation of the model.

## Input files

### Physical model configuration: `glm.nml`

The file `glm.nml` is the main configuration file for the physical model, and some details related to the FABM coupling. The `nml` file includes detailed description of the different namelist options for each block; if these value are not present default values will be assumed. It is a namelist file with blocks for:

- `&glm_setup:` General simulation info
- `&fabm_setup:` Details about the FABM coupling
- `&time:` Time controls
- `&morphometry:` Lake morphometric information
- `&output:` Output file details
- `&init_profiles:` Initial profiles
- `&meteorology:` Information about surface forcing and meteorology data
- `&inflows:` Information about inflows
- `&outflows:` Information about outflows

### Biogeochemical model configuration: fabm.nml

The file `fabm.nml` is the main file to configure the simulated FABM models/modules, and the relevant model parameters. It includes a compulsory section at the top of the file to select the models/modules to be included in the simulation. Note that the order of the selected models must be in an order that allows FABM to set the dependencies in a logical and consecutive order. In the example below a range of different modules are selected:

```
&fabm_nml
models = ! Example Modules
          'examples_npzd_nut','examples_npzd_det',
          'examples_npzd_phy','examples_npzd_zoo',
! AED Modules
          'aed_sedflux',
          'aed_oxygen',
          'aed_carbon',
          'aed_silica',
          'aed_nitrogen',
          'aed_phosphorus',
          'aed_organic_matter',
          'aed_phytoplankton',
          'aed_geochemistry'
/

```

In this example, the simulation would include four of the generic ‘npzd’ modules and nine of the AED modules. They are ordered such that the zooplankton in `examples_npzd_zoo` are able to depend on the phytoplankton in `examples_npzd_phy` who depend on the nutrients in `examples_npzd_nut`. Similarly the phytoplankton in the `aed_phytoplankton` model are dependent on the nutrients from `aed_nitrogen` and `aed_phosphorus` and so the order they are listed must reflect this.

As FABM registers the selected models, it will then parse the remainder of the file to find model specific parameter and configuration information. Note that FABM reads the file and requires model-specific parameter blocks to be in the file in the order they are configured. For a list of variables simulated by each of the AED modules, see Table 4.

One of the strengths of FABM is the ability to link a model to state variables in another model. As an example, the `aed_phytoplankton` module is dependent on nutrients from the nutrient modules and recycles material back to the organic matter modules, as shown in:

```
&aed_phytoplankton
num_phytos = 3
the_phytos = 3,7,8
p_excretion_target_variable  ='aed_organic_matter_dop'
n_excretion_target_variable  ='aed_organic_matter_don'
c_excretion_target_variable  ='aed_organic_matter_doc'
si_excretion_target_variable = ''
p_mortality_target_variable = 'aed_organic_matter_pop'
n_mortality_target_variable = 'aed_organic_matter_pon'
c_mortality_target_variable = 'aed_organic_matter_poc'
si_mortality_target_variable = ''
p1_uptake_target_variable   ='aed_phosphorus_frp'
n1_uptake_target_variable   ='aed_nitrogen_nit'
n2_uptake_target_variable   ='aed_nitrogen_ammonium'
si_uptake_target_variable   ='aed_silica_rsi'
do_uptake_target_variable   ='aed_oxygen_oxy'
c_uptake_target_variable    ='aed_carbon_dic'
/

```

Here the model is configured to add excretion of P to the DOP pool in `aed_organic_matter`, however this could easily be configured to return it directly to the FRP pool of `aed_phosphorus`, or even the `examples_npzd_nut` pool in the above configuration if desired. If a target variable is not required the simply place ‘’ as the target and the flux will still occur but not be added to a dependent module such as in the above example for silica.

### Meteorology: `met.csv`

The meteorological conditions are provided as a daily time-series of data with a fixed number of columns, as outlined in Table 14. Sub-daily inputs are also supported if the “subdaily” flag is enabled in the `glm.nml` file. If the flag is false then the user must provide daily data, and if true then the user must supply data at the frequency of the time-step chosen for the model operation.

The file contains seven compulsory columns, and several optional columns after these depending on the user-defined configuration switches for `snow_sw` and `rain_sw` in the `glm.nml` file.

**Table 14: Flow diagram showing the files required for operation of the model.**

Met.csv column	Units	Description
(1) <i>TIME</i>	YYYY-MM-DD	Date
(2) <i>SHORTWAVE RADIATION</i>	W/m <sup>2</sup>	Daily average shortwave radiation.  Note that the daily value is internally distributed to a sub-daily time step by assuming an idealized diurnal cycle.
(3) <i>LONGWAVE RADIATION</i>	W/m <sup>2</sup> if <code>lw_type = LW_IN</code> or <code>LW_NET</code> or 0 – 1 if <code>lw_type = LW_CC</code>	Longwave radiation input is either direct incident intensity, net longwave flux, or estimated from cloud cover fraction.
(4) <i>AIR TEMPERATURE</i>	°C	Daily average air temperature 10m above the water surface
(5) <i>RELATIVE HUMIDITY</i>	%	Daily average relative humidity (0-100%) 10m above the water surface.
(6) <i>WIND SPEED</i>	m/s	Daily average wind speed 10m above the water surface
(7) <i>RAINFALL</i>	m/day	Daily rainfall depth
(8) <i>SNOWFALL (optional)</i>	m/day	Daily snowfall depth (optional – include if <code>snow_sw</code> is T)
(9-14) <i>RAINFALL WQ DEPOSITION CONCENTRATIONS (optional)</i>	mg/L	... (optional – include if <code>rain_sw</code> is T)

#### Inflows: inflows.csv

Any number of inflows can be simulated by the model with the configuration and filenames set in the `glm.nml` file. For each inflow there is an associated inflow file of the format outlined in Table 15. At this stage the file only accepts daily data as the inflow calculation is done once a day. It contains four compulsory columns for time, flow, temperature and salinity, and then optional columns for FABM constituents.

**Table 15: Flow diagram showing the files required for operation of the model.**

Inflow.csv column	Units	Description
(1) TIME	YYYY-MM-DD	Date
(2) INFLOW	ML/day	Daily flow rate. Users can convert data from $m^3/s$ by multiplying by 86.4.
(3) STREAMFLOW TEMPERATURE	°C	Average daily streamflow temperature
(4) STREAMFLOW SALINITY	mg/L	Average daily streamflow salinity
(5 ... $n_{WQ}+4$ ) STREAMFLOW FABM PARAMETER CONCENTRATIONS	mmol/m <sup>3</sup>	Average daily streamflow FABM constituent concentrations.

#### Outflows: outflows.csv

Any number of outflow fluxes can be configured and these are set as consecutive columns in the file `outflows.csv` (Table 16). Only daily flow rates are required and FABM variables are not required.

**Table 16: Flow diagram showing the files required for operation of the model.**

Outflow.csv column	Units	Description
(1) TIME	YYYY-MM-DD	Date
(2 ... $n_{OUT}+1$ ) OUTFLOW	ML/day	Daily outflow rates of each outflow

### Biogeochemical model parameter files

Three of the FABM-AED modules require extra `nml` or `dat` files that each contain a database of parameters required for those modules. Note that not all parameters in these files are used by the modules, but these contain an extensive library of potential species parameters that may be selected when the modules are configured.

#### `aed_phyto_pars.nml`

This file contains a namelist block “`&phyto_data`” that has numerous columns that match the list of phytoplankton parameters included in Table X in the above section and is compulsory if `aed_phytoplankton` is enabled. Note that to be read correctly this must include all columns. Each row is a specific parameter set that may correspond to a particular species or functional group. This file may be read easily in excel using commas as the delimiter.

#### `aed_zoop_pars.nml`

As above, this file contains a namelist block “`&zoop_params`” that has numerous columns that match the list of zooplankton parameters included in Table X in the above section, and is compulsory if `aed_zooplankton` is enabled. Note that to be read correctly this must include all columns. Each row is a specific parameter set that may correspond to a particular species or functional group. This file may be read easily in excel using commas as the delimiter.

#### `aed_geochem_pars.dat`

This file is not a namelist file but rather a series of chemical expressions with reaction constants in the above section and is compulsory if `aed_geochemistry` is enabled. The model will parse this file and select relevant expressions required for the model setup based on the selected dissolved and mineral parameters in the `&aed_geochemistry` of `fabm.nml`. The file includes three main sections, namely: `COMPONENTS`, `SPECIES` and `PHASES`, and they must be present in that order. The file ends with the `ENDFILE` keyword. Note that the these expressions and constants are originally based on the PHREEQC wateq4f geochemical database constants (originally based on Nordstrom et al).

#### `aed_sediment_swibc.dat`

This file is not a namelist file but rather a dynamic time-series of bottom water conditions (dissolved concentrations and particulate flux rates) if the sediment diagenesis model is on and driven by external conditions rather than internally predicted values from other FABM modules. It is compulsory if `aed_seddiagenesis` model is enabled and the Sediment-Water Interface (SWI) boundary condition option is 10 (ie., `ibc2=10`).

## Running the model

The model may be run by navigating to the directory where the `glm.nml` and `fabm.nml` files are and executing the model executable `glm.exe`. This can be located in different directory and added to the system path if desired.

Windows users may wish to add the command into a `glm.bat`:

```
..\bin\glm.exe >glm.log
```

which will create a file that can simply be double-clicked from windows explorer. The model will output to the netcdf and/or csv files which can then be plotted.

## Outputs and post-processing

The model includes several types of outputs, including the NETCDF file, an optional csv time-series file at a certain point, and an optional live contour plot as the model runs to enable the modeller to monitor simulation progress.

## Live output plotting: plots.nml

If the model is run with the optional command line argument “--xdisp” then the model will display live plots (Figure 6) of output parameters.

```
..\bin\glm.exe --xdisp > glm.log
```

The number of plots, parameters to plot and the colour bar limits are set in the file plots.nml.

```
&plots
nplots = 4
plot_width = 400
plot_height = 200
title = 'Temperature', 'Salinity', 'Oxygen', 'Greens'
vars = 'temp', 'salt', 'aed_oxygen_oxy', 'aed_phytoplankton_green'
min_z = 0.0, 0.0, 0.0, 0.0
max_z = 27.0, 0.91, 800.0, 20.0
/
```

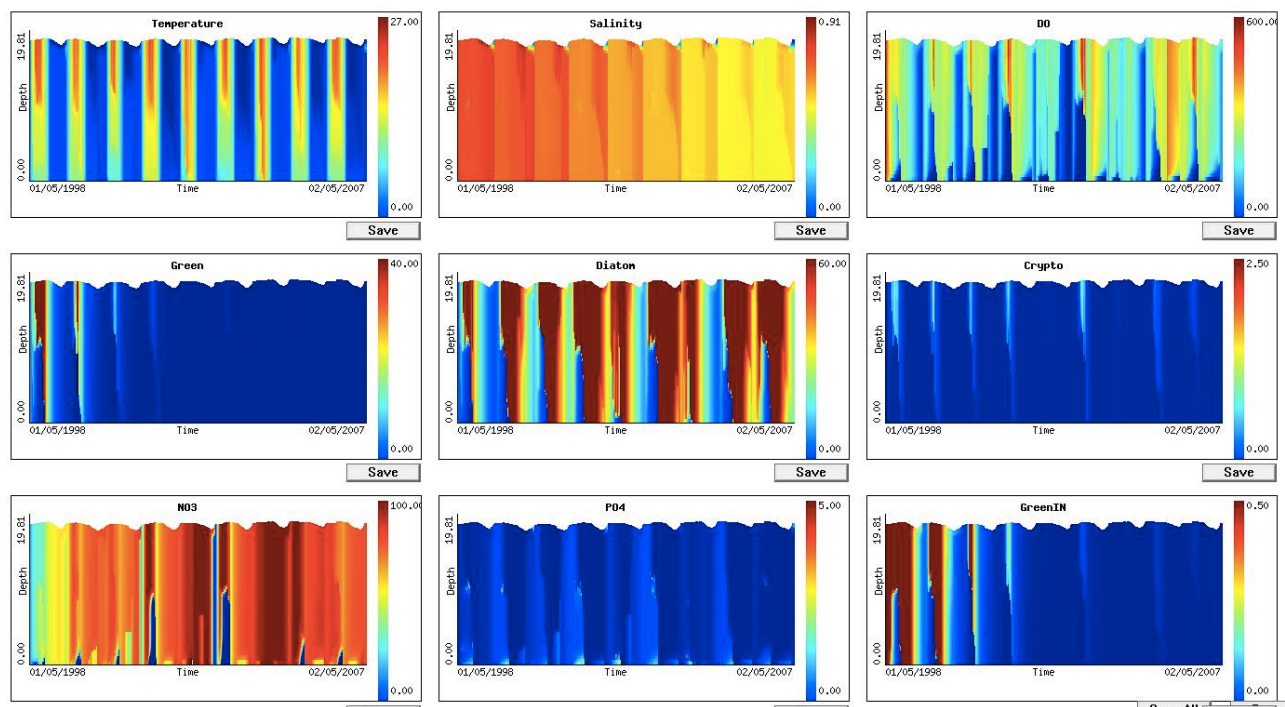


**Figure 6: Example outputs from the model using the in-built runtime plots.**

## Plotting in EXCEL

For simple time-series plots, the user can configure outputs from the model directly to a csv file for a certain depth (defined relative to the bottom, or from the surface), and this information is defined in the glm.nml “&output” section. The columns to plot are also listed here and are user-definable, though must be simulated.

Users also get a general lake.csv file that includes general lake information predicted by the model including the lake depth, volume, lake number and other diagnostic parameters.

## Plotting with PyNCview

Some one please write me!

## Plotting with R Studio

Some one please write me!

## Plotting in MATLAB

For more advanced or customised plots, then the user may load the `output.nc` NETCDF file into MATLAB. Recent versions of MATLAB (MATLAB 2011a or after) natively support NETCDF and can load the file directly. An example MATLAB script for plotting is shown below: and produces figures as in Figure X.

```
% -- Sim and output location
foldername = '../MyGLMSim/';
outname    = '../MyGLMSim/figures/';
mkdir([outname]);

% -- Get list of simulated names
varNames = names_ncdf([foldername,'output.nc']);

% -- Choose sub-set of variable list to plot as required
varsToPlot = varNames([20:60]);

% -- Load GLM NetCDF file
glmdata = nldncGLM([foldername,'/output.nc'])

% -- Plot each and save
for ii = 1:length(varsToPlot)
    newFig = plotGLM(varsToPlot{ii}, glmdata);

    figName = [outname,'/', varsToPlot{ii},'.png'];
    print(gcf,'-dpng', figName,'-opengl');
    close all
end
```

For this users must have “`nldncGLM.m`” and “`plotGLM.m`” in their path. A simple GLM-FABM plotting MATLAB GUI is also available (Figure 7), as part of a GLM toolbox.

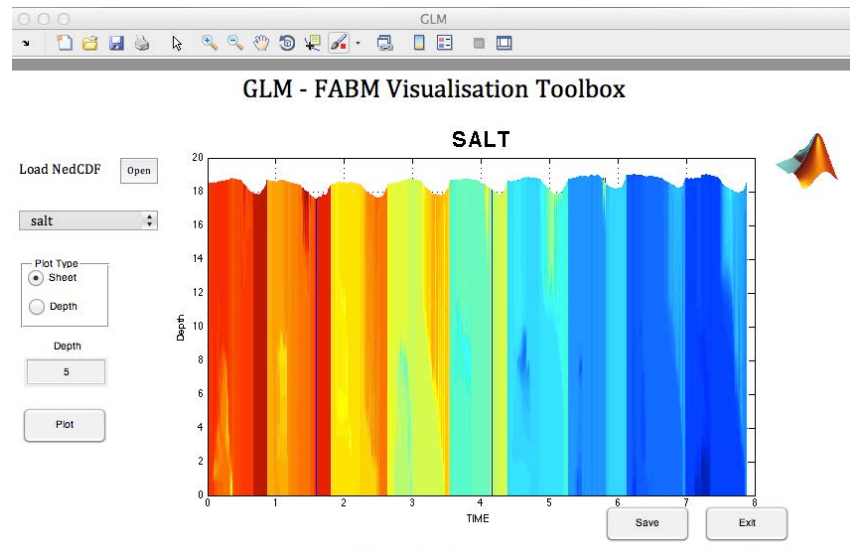


**Figure 7: MATLAB GUI for plotting GLM `output.nc` files.**

## Outputting model results to *LakeAnalyzer*

<Note; under development>

Model simulation results can be optionally written to the input file for the GLEON LakeAnalyzer program (Read et al 2011; gleon.lakeanalyzer.org).

<Note; under development>

# References

---

- Ambrose, R.B. Jr., Wool, T.A., Conolly, J.P., and Scahnz, R.W.. 1988. A Hydrodynamic and Water Quality Model: Model Theory, Users Manual, and Programmers manual: WASP4 Environmental Research Laboratory, US EPA, EPA 600/3-87/039, Athens, GA.
- Arhonditsis, G.B., Adams-Vanharn, B.A., Nielsen, L., Stow, C.A., and Reckhow, K.H., 2006. Evaluation of the current state of mechanistic aquatic biogeochemical modeling: citation analysis and future perspectives. *Environ. Sci. Technol.*, **40**, 6547-6554.
- Arhonditsis, G.B., M.T. Brett. 2004. Evaluation of the current state of mechanistic aquatic biogeochemical modeling. *Marine Ecology Progress Series*, **271**: p. 13–26.
- Bruce, L.C., Hipsey, M.R. and Cook, P.M., Quantification of sediment and water processing of nitrogen in a periodically anoxic urban estuary using a 3D hydrodynamic-biogeochemical model. Submitted to *Journal of Soils and Sediments*.
- Bruce LC, Hamilton DP, Imberger J, Gal G, Gophen M, Zohary T, Hambright KD, 2006. A numerical simulation of the role of zooplankton in C, N and P cycling in Lake Kinneret, Israel. *Ecol. Model.* **193**:412-436.
- Broekhuizen, N., Rickard, G. J., Bruggeman, J. & Meister, A. 2008. An improved and generalized second order, unconditionally positive, mass conserving integration scheme for biochemical systems. *Applied Numerical Mathematics* 58:319–40.
- Bruggeman, J. 2011. D2.14 Users guide and report for models in the MEECE library – Framework for Aquatic Biogeochemical Models (FABM). Report for the EC FP7 MEECE project 212085. 57pp.
- Burchard H et al. 2005. Application of modified Patankar schemes to stiff biogeochemical models, *Ocean Dyn*, **55**: 326-37
- Burchard, H., Bolding, K., Kuhn, W., Meister, A., Neumann, T. & Umlauf, L. 2006. Description of a flexible and extendable physical-biogeochemical model system for the water column. *Journal of Marine Systems* 61: 180-211.
- Chao, X., Jia, Y., Shields, F.D., Wang, S.S.Y., and Cooper, C.M., 2010. Three-dimensional numerical simulation of water quality and sediment-associated processes with application to a Mississippi Delta lake. *Journal of Environmental Management* **91**: 1456 – 1466.
- Coles, J.F. and R.C. Jones. 2000. Effect of temperature on photosynthesis-light response and growth of four phytoplankton species isolated from a tidal freshwater river. *J. Phycology*, **36**: 7-16.
- Droop, M.R. 1974. The nutrient status of algal cells in continuous culture. *J. Mar. Biol. Assoc. UK*, **54**: 825–855.
- Fasham, M.J.R., Ducklow, H.W. & Mckelvie, S.M., 1990. A nitrogen-based model of plankton dynamics in the oceanic mixed layer. *J. Mar Res* 48: 591-639
- Gal, G., Hipsey, M.R., Paparov, A., Makler, V. and Zohary, T., 2009. Implementation of ecological modeling as an effective management and investigation tool: Lake Kinneret as a case study. *Ecol. Model.*, **220**: 1697-1718.
- Kilminster et al., 2011. Unpublished data.
- Romero, J.R., Antenucci, J.P., & Imberger, J. 2004. One- and Three- Dimensional biogeochemical Simulations of Two Differing Reservoirs. *Ecol. Model.*.
- Riley, J.P. & Skirrow, G.. 1974. Chemical Oceanography Academic Press, London.
- Robarts, R.D. and T. Zohary. 1987. Temperature effects on photosynthetic capacity, respiration and growth rates of bloom forming cyanobacteria. *N.Z. J Mar. Freshwater Res.* **21**: 391-399.
- Schladow, S.G. & Hamilton, D.P. 1997 Water quality in lakes and reservoirs. Part II Model calibration, sensitivity analysis and application. *Ecol. Model.* **96**: 111–123.
- Rhee, G.Y. & Gotham, E.J. 1981 The effect of environmental factors on phytoplankton growth: temperature and the interactions of temperature with nutrient limitation. *Limnol. Oceanogr.* **26**, pp. 635–648.
- Jellison, R. & Melack, J.M. 1993. Meromixis and vertical diffusivities in hypersaline Mono Lake, California. *Limnol. Oceanogr.* **38**: 1008–1019.
- Kromkamp, J. & Walsby, A.E. 1990. A computer model of buoyancy and vertical migration in cyanobacteria. *J. Plankton Res.* **12**: 191–183.
- Griffin, S.L., Herzfeld, M., Hamilton, D.P., 2001. Modelling the impact of zooplankton grazing on phytoplankton biomass during a dinoflagellate bloom in the Swan River Estuary, Western Australia. *Ecological Engineering*, **16**: 373-394.
- Hamilton, D.P. & Schladow, S.G. 1997. Water quality in lakes and reservoirs. Part I Model description. *Ecol. Model.* **96**: 91–110.
- Hipsey, M.R., Salmon, S.U., Aldridge, K.T. and Brookes, J.D., 2010. Impact of hydro-climatological change and flow regulation on physical and biogeochemical dynamics of the Lower River Murray, Australia. *8th International Symposium on Ecohydraulics (ISE2010)*, September, 2010, Korea.
- Kruger, G.H.J. and J.N. Eloff. 1977. The influence of light intensity on the growth of different *Microcystis* isolates. *J. Limnol. Soc. Sth Africa*. **3**: 21-25.
- Imberger, J. and J.C. Patterson. 1981. A dynamic reservoir simulation model-DYRESM:5. In "Transport Models for Inland and Coastal Waters." H.B. Fisher(ed). Academic Press, New York. : 310-361.
- Mooij, W.M., Trolle, D., Jeppesen, E., Arhonditsis, G., Belolipetsky, P.V., Chitamwebwa, D.B.R., Degermendzhy, A.G., DeAngelis, D.L., De Senerpont Domis, L.N., Downing, A.S., Elliott, A.E., Fragoso Jr, C.R., Gaedke, U., Genova, S.N., Gulati, R.D., Håkanson, L.,

- Hamilton, D.P., Hipsey, M.R., Hoen, J., Hülsmann, S., Los, F.J., Makler-Pick, V., Petzoldt, T., Prokopkin, I.G., Rinke, K., Schep, S.A., Tominaga, K., Van Dam, A.A., Van Nes, E.H., Wells, S.A., Janse, J.H., 2010. Challenges and opportunities for integrating lake ecosystem modelling approaches, *Aquatic Ecology*, **44**: 633–667.
- Petrone K.C. Richards, J.S. and Grierson, P.F., 2009. Bioavailability and composition of dissolved organic carbon and nitrogen in a near coastal catchment of south-western Australia. *Biogeochemistry*, **92**: 27-40.
- Smith, C.S., Haese, R.R. and Evans, S. 2010. Oxygen demand and nutrient release from sediments in the upper Swan River estuary. Geoscience Australia Record, 2010/28. Commonwealth Government, Canberra.
- Smith, C.S., Murray, E.J., Hepplewhite, C. and Haese, R.R. (2007. Sediment water interactions in the Swan River estuary: Findings and management implications from benthic nutrient flux surveys, 2000-2006. Geoscience Australia Record 2007/13.
- Spillman, C.M., Hamilton, D.P., Hipsey, M.R. and Imberger, J., 2008. A spatially resolved model of seasonal variations in phytoplankton and clam (*Tapes philippinarum*) biomass in Barbamarco Lagoon, Italy, *Estuarine, Coastal and Shelf Science*, **79**: 187-203.
- Spillman, C.M., Imberger, J., Hamilton, D.P., Hipsey, M.R. and Romero, J.R., 2007. Modelling the effects of Po River discharge, internal nutrient cycling and hydrodynamics on biogeochemistry of the Northern Adriatic Sea. *Journal of Marine Systems*, **68**: 127-200.
- Talling, J. F. 1957. The phytoplankton population as a compound photosynthetic system. *New Phytol.* **56**: 133-149
- Trolle, D., Hamilton, D.P., Hipsey, M.R., Bolding, K., Bruggeman, J., Mooij, W. M., Janse, J. H., Nielsen, A., Jeppesen, E., Elliott, J. E., Makler-Pick, V., Petzoldt, T., Rinke, K., Flindt, M. R., Arhonditsis, G.B., Gal, G., Bjerring, R., Tominaga, K., Hoen, J., Downing, A. S., Marques, D. M., Fragoso Jr, C. R., Søndergaard, M. and Hanson, P.C. 2012. A community-based framework for aquatic ecosystem models. *Hydrobiologia*, **683**(1): 25-34.
- Wanninkhof, R.. 1992. Relationship between windspeed and gas exchange over the ocean. *J. Geophys. Res. (Oceans)* **97**(C5): 7373–7382.
- Webb, W.L., Newton, M., & Starr, D. 1974. Carbon dioxide exchange of *Alnus rubra*: a mathematical model. *Oecologia* **17**: 281–291.
- Yeates, P.S. and Imberger, J. 2004. Pseudo two-dimensional simulations of internal and boundary fluxes in stratified lakes and reservoirs. *Int. J. Riv. Basin Res.* **1**: 1-23.